Bioorg.Med.2007

DATASET · JULY 2013

READS
30

8 AUTHORS, INCLUDING:

Nilgün Karali
Istanbul University
42 PUBLICATIONS **514** CITATIONS
SEE PROFILE

Fatma Kandemirli
Kastamonu Üniversitesi
86 PUBLICATIONS **1,157** CITATIONS
SEE PROFILE

Suheyla Ozbey
Hacettepe University
124 PUBLICATIONS **827** CITATIONS
SEE PROFILE

Vasyl Kovalishyn
Institute of Bioorganic Chemistry and Petro…
52 PUBLICATIONS **351** CITATIONS
SEE PROFILE

Available online at www.sciencedirect.com
ScienceDirect
Bioorganic & Medicinal Chemistry 15 (2007) 5888–5904
Bioorganic & Medicinal Chemistry

Synthesis and structure–antituberculosis activity relationship of 1*H*-indole-2,3-dione derivatives

Nilgün Karalı,[a,*] Aysel Gürsoy,[a] Fatma Kandemirli,[b] Nathaly Shvets,[c] F. Betül Kaynak,[d] Süheyla Özbey,[d] Vasyl Kovalishyn[e] and Anatholy Dimoglo[c,f]

[a]*Istanbul University, Faculty of Pharmacy, Department of Pharmaceutical Chemistry, 34116 Beyazıt, Istanbul, Turkey*
[b]*Kocaeli University, Department of Chemistry, 41100 Kocaeli, Turkey*
[c]*Gebze Institute of Technology, PK-141, 41400 Gebze, Kocaeli, Turkey*
[d]*Hacettepe University, Department of Physics Engineering, 06532 Beytepe, Ankara, Turkey*
[e]*Institute of Bioorganic Chemistry & Petrochemistry, 02660 Kyiv, Ukraine*
[f]*Institute of Applied Physics, Academy of Sciences of Moldova, MD-2028 Kishinev, Republic of Moldova*

Received 11 December 2006; revised 22 May 2007; accepted 30 May 2007
Available online 2 June 2007

Abstract—New series of 5-fluoro-1*H*-indole-2,3-dione-3-thiosemicarbazones **2a**–**k** and 5-fluoro-1-morpholino/piperidinomethyl-1*H*-indole-2,3-dione-3-thiosemicarbazones **3a**–**r** were synthesized. The structures of the synthesized compounds were confirmed by spectral data, elemental and single crystal X-ray diffraction analysis. The new 5-fluoro-1*H*-indole-2,3-dione derivatives, along with previously reported 5-nitro-1*H*-indole-2,3-dione-3-thiosemicarbazones **2l**–**v**, 1-morpholino/piperidinomethyl-5-nitro-1*H*-indole-2,3-dione-3-thiosemicarbazones **4a**–**l**, and 5-nitro-1*H*-indole-2,3-dione-3-[(4-oxo-1,3-thiazolidin-2-ylidene)hydrazones] **5a**–**s**, were evaluated for in vitro antituberculosis activity against *Mycobacterium tuberculosis* H37Rv. Among the tested compounds, 5-nitro-1*H*-indole-2,3-dione-3-thiosemicarbazones (**2p**, **2r**, and **2s**) and its 1-morpholinomethyl derivatives (**4a**, **4e**, **4g**, and **4i**) exhibited significant inhibitory activity in the primary screen. The antituberculosis activity of molecules with diverse skeletons was investigated by means of the Electronic-Topological Method (ETM). Ten pharmacophores and ten anti-pharmacophores that have been found by this form the basis of the system capable of predicting the structures of potentially active compounds. The forecasting ability of the system has been tested on structures that differ from those synthesized. The probability of correct identification for active compounds was found as equal to 93% in average. To obtain the algorithmic base for the activity prediction, Artificial Neural Networks were used after the ETM (the so-called combined ETM–ANN method). As the result, only 9 pharmacophores and anti-pharmacophores were chosen as the most important ones for the activity. By this, ANNs classified correctly 94.4%, or 67 compounds from 71.

1. Introduction

Tuberculosis (TB) is a contagious disease with high mortality worldwide. The statistics indicate that 3 million people worldwide die annually from complication of TB[1] and there are estimated 8 million of new cases each year, 95% of which occur in developing countries.[2] Drugs such as isoniazid (INH) and rifampicin have historically been successful in the treatment of TB infections. In recent history, however, poor compliance with the prolonged and complicated chemotherapeutic regimens currently used to treat the disease, in conjunction with the advent of the AIDS epidemic and the increased mobility of human populations, has led to the emergence of numerous multidrug-resistant *Mycobacterium tuberculosis* strain.[3] Resistance to frontline therapeutics, most notably INH and rifampicin, results in treatment of patients with second-line agents. Among these second tier drugs for the treatment of multidrug-resistant TB, thiacetazone (Fig. 1) has been widely used in Africa and South America. It has been found to be a very effective drug for the treatment of TB when administered in combination with INH.[4]

Recently, a number of thiacetazone derivatives have been synthesized and described for their activity against *M. tuberculosis*, *M. avium*, and other mycobacterial species.[5–7] Results indicate that some

Keywords: 1*H*-Indole-2,3-diones; Antituberculosis activity; Structure–activity relationships; Electronic-topological method (ETM).
* Corresponding author. Fax: +90 212 440 0252; e-mail: karalin@istanbul.edu.tr

0968-0896/$ - see front matter © 2007 Elsevier Ltd. All rights reserved.
doi:10.1016/j.bmc.2007.05.063

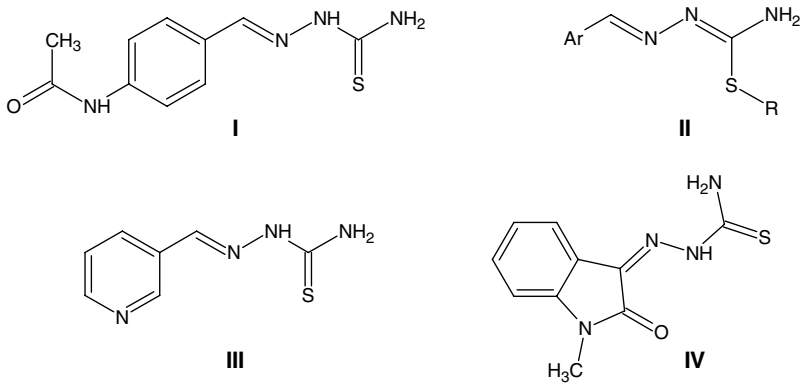

Figure 1. Structures of thiacetazone (**I**), *S*-alkylisothiosemicarbazones (**II**), SRI-286 (**III**), and methisazone (**IV**).

S-alkylisothiosemicarbazones and SRI-286 (Fig. 1) can be useful in the therapy and prophylaxis of mycobacteria infections and can represent a template for the development of novel antimycobacterial drugs.

1*H*-Indole-2,3-dione is an endogenous compound identified in humans and its effect has been studied in a variety of systems. Biological properties of 1*H*-indole-2,3-dione include a range of actions in the brain and offer protection against certain types of infections. Methisazone (Fig. 1) plays an important role as prophylactic agent against several viral diseases.[8]

In recent years, Schiff and Mannich bases of 1*H*-indole-2,3-diones are reported to exhibit broad-spectrum chemotherapeutic properties such as antiviral,[9–11] anti-TB,[12,13] antifungal, and antibacterial activities.[14,15] Investigation of the structure–activity relationships in 1*H*-indole-2,3-dione derivatives revealed that 5-halogenation,[12–15] N-alkylation,[16,17] N-Mannich base,[13–15] and 3-thiosemicarbazone formation[10,11,14] were effective in causing a marked rise in activity against various bacteria, fungi, and virus. Moreover, cyclization of 1*H*-indole-2,3-diones to 4-thiazoline,[12] 4-thiazolidinone,[18] and pyridazinoindole[17] was efficient in increasing antimicrobial activity.

Because of all the said and as a continuation of our works on 1*H*-indole-2,3-dione derivatives, we have synthesized 5-fluoro-1*H*-indole-2,3-dione-3-thiosemicarbazone derivatives, in order to obtain new and more potent anti-TB compounds. These new 5-fluoro-1*H*-indole-2,3-dione derivatives along with previously reported 5-nitro-1*H*-indole-2,3-dione derivatives[19,20] were evaluated for in vitro anti-TB activity against *M. tuberculosis* H37Rv.

Previously, structure–activity relationships (SAR) were studied for a series of novel 5-aryl-2-thio-1,3,4-oxadiazo[21] and 2,5-disubstituted-1,3,4-thiadiazoles[22] which were synthesized and screened for in vitro anti-TB activity against *M. tuberculosis* H37Rv. This systematic SAR study was performed through the application of the ETM approach to the series of compounds with experimentally measured anti-TB activity.

As known, the better is the description of molecules in terms of structural parameters related to the activity in view, the better are results on pattern recognition and separation of molecules by their activities. The ETM is capable of taking into account any individual properties of atoms and bonds, and this fact may be crucial for revealing details of interactions between a biological receptor and an active molecule. The ETM was used here for the structure–anti-TB activity study in the series of molecules with quite diverse skeletons.

2. Results and discussion

2.1. Chemistry

In this study, 5-fluoro-1*H*-indole-2,3-dione (**1a**) reacted with different N-substituted thiosemicarbazides in ethanol containing a catalytic amount of sulfuric acid to give the corresponding 5-fluoro-1*H*-indole-2,3-dione-3-thiosemicarbazones (**2a**–**k**). 5-Fluoro-1-morpholino/piperidinomethyl-1*H*-indole-2,3-dione-3-thiosemicarbazones (**3a**–**r**) were synthesized from the consecutive treatment of **2a**–**k** with formaldehyde solution and morpholine or piperidine (Scheme 1).

The structures of the synthesized compounds were confirmed by elemental analyses and spectral (IR, ^{1}H NMR, ^{13}C NMR-APT, HETCOR-2D, and LCMS-APCI) data. The IR spectra of **2** and **3** showed absorption bands in the 3371–3171, 1694–1687, and 1154–1130 cm^{-1}, and 3309–3211, 1701–1686 and 1158–1130 cm^{-1} regions resulting from the NH, C=O, and C=S functions, respectively. ^{13}C NMR-APT of **2d**, **3g**, and **3h**, and HETCOR spectra of **2b**, **2e**, **3c**, and **3d** supported the IR findings and displayed signals at δ 162.06–163.13, 138.87–140.34 and 177.06–177.31 ppm which showed that there was no ^{13}C–^{1}H connection attributed to the C=O, C=N, and C=S functions. The ^{1}H NMR spectra of **2a**–**k** displayed the NH protons of the thiosemicarbazone moiety (δ 8.87–11.09 and 12.45–12.89 ppm) and the indole NH proton (δ 11.09–11.30 ppm) as three separate signals. The indole C_7, C_6, and C_4 protons appeared as double doublets, double triplets, and double doublets with the ^{1}H–^{1}H and ^{1}H–^{19}F connections at δ 6.78–6.95, 7.03–7.24, and

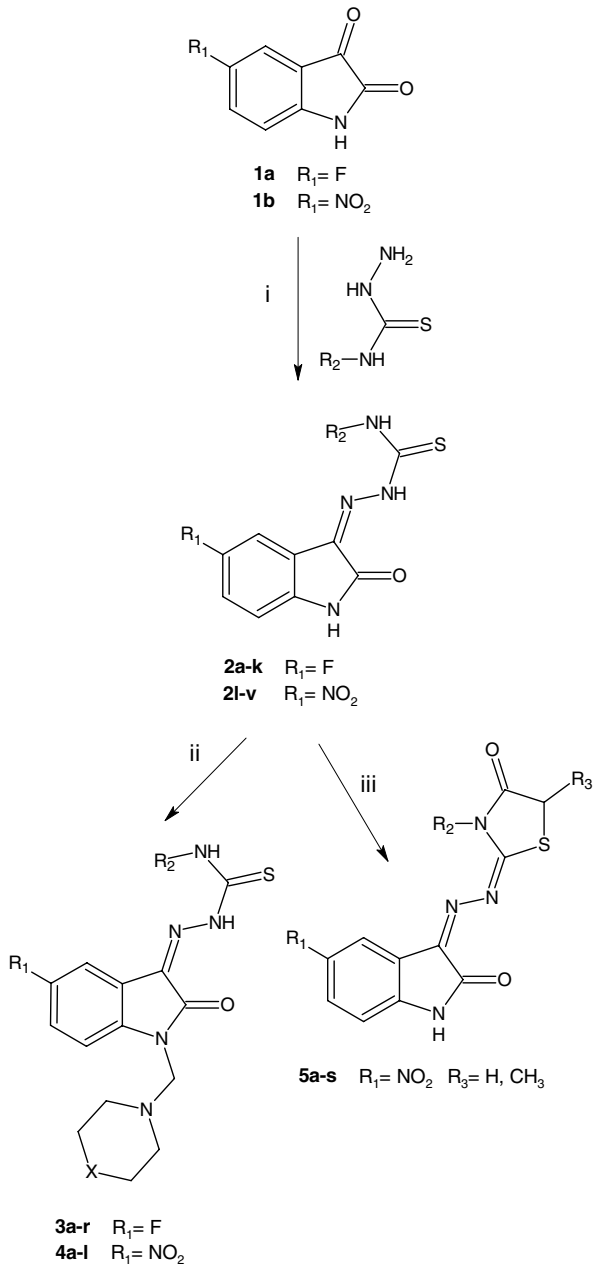

Scheme 1. Reagents and conditions: (i) EtOH, reflux, 5 h; (ii) morpholine or piperidine, 37% HCHO, absolute EtOH, stir, rt, 10 h or reflux, 4 h; (iii) ethyl bromoacetate or ethyl 2-bromopropionate, anhydrous sodium acetate, absolute EtOH, reflux, 4 h.

7.44–7.65 ppm on the basis of HETCOR data. Observation of only two NH signals assigned to the thiosemicarbazone moiety (δ 8.92–10.93 and 12.36–12.65 ppm) and of a singlet due to N–CH_2–N function (δ 4.46–4.51 ppm and δ 61.81–62.51 ppm) and of signals attributed to morpholine or piperidine ring in the ^{1}H and ^{13}C NMR spectra of **3** provided support for N-Mannich base formation. While in the ^{1}H NMR spectra of **2b**, **3c**, and **3d** were observed ethyl CH_2 protons at 3.66 ppm, ethyl CH_2 carbons were observed together with DMSO in the ^{13}C NMR spectra. HETCOR spectra of **2b**, **3c**, and **3d** supported the ^{1}H and ^{13}C NMR findings. Protons of the cyclohexyl moiety in the ^{1}H NMR spectra of **2e** and **3i** showed as the axial and equivatorial protons on the basis of HETCOR. The indole carbons in the spectra of **2** and **3** which explicitly showed the ^{13}C–^{19}F connections were observed as separate doublets with evident connection constant. LCMS-APCI of **2b**, **2d**, **2f**, **2g**, **2h**, **2j**, **3g**, **3m**, **3n**, and **3q** chosen as prototypes displayed molecular ions with different intensities. The major fragmentation pathway involved concomitant breaking of the NH–CS bond yielding fragments [*m*/*z* 178 (−) and 180 (+)] characteristic for the 5-fluoro-1*H*-indole-2,3-dione-3-hydrazone moiety.

2.2. X-ray analysis

The X-ray structures of **3e** and **3f** were determined in order to confirm the assigned structures and to establish conformations of the molecules. Relevant crystal data and details of the structure determinations are given in Table 1, and selected geometric parameters are given in Table 2. ORTEP drawings of structures with atomic numbering are shown in Figures 2 and 3. As expected, the indole moiety is nearly planar in both molecules. The maximum displacements from the least-squares plane for all nine atoms contained in the ring are −0.028(3) for C2 (**3e**) and 0.007(3) Å for C8 (**3f**). In **3e**, the morpholine ring is taken in a chair shape having spherical polar set values[23] $Q = 0.640(3)$ Å, $\theta = 175.6(3)°$, and $\varphi = 3(4)°$. Atoms O2 and N2 are displaced from the C10/C11/C12/C13 mean plane by 0.701(2) and −0.788(2) Å, respectively. Similarly, in **3f** the piperidine (N2/C10/C11/C12/C13/C14) ring adopts the chair conformation. The puckering parameters of this ring are $Q = 0.581(4)$Å, $\theta = 0.0(4)°$, and $\varphi = 63(12)°$. N2 and C12 atoms are displaced from the C10/C11/C13/C14 mean plane by −0.672(2) and 0.677(4) Å, respectively.

As can be seen from Figures 2 and 3, the molecules are not planar. The dihedral angles between the morpholine or piperidine rings and indole–thiosemicarbazone system in **3e** and **3f** are 86.2(1) and 82.1(1)°, respectively. The approximate planarity of indole–thiosemicarbazone system is due to the intramolecular hydrogen bonds, existence in the molecules. In both molecules, the intra- and intermolecular N–H···O, C–H···O, and N–H···N hydrogen bonds are observed (Table 3). In **3e**, dimeric units are formed through the C–H···F interactions of the phenyl rings and dimers of molecules linked through the C–H···O hydrogen bonds which extend along the *c* axis (Fig. 4). In **3f**, N–H···S intermolecular contacts also generate infinite chains along *c* axis (Fig. 5).

In addition, there are three intermolecular C–H···π interactions involving the indole heterocycle that is present in both molecules. In molecule **3e**, one of the C–H···π interactions happens between pyrrole ring and N5 atom, and two others are related with the phenyl ring of the indole heterocycle and the hydrogen atoms

Table 1. Crystal data and structure refinement parameters for **3e** and **3f**

Compound	**3e**	**3f**
Formula	$C_{17}H_{20}FN_5O_2S$	$C_{18}H_{22}FN_5OS$
Model molecular weight	377.44	375.47
Crystal system	Triclinic	Monoclinic
Space group	$P\bar{1}$	$P2_1/c$
Unit cell dimensions		
a (Å)	6.3291(8)	9.1286(5)
b (Å)	10.0080(13)	19.0680(9)
c (Å)	14.4884(19)	11.4206(5)
α (°)	82.498(11)	—
β (°)	85.569(11)	106.955(5)
γ (°)	90.742(11)	—
V (Å^3)	906.9(2)	1901.51(16)
D_{calc} (g cm^{-3})	1.382	1.312
Z	2	4
Temperature (°K)	293(2)	293(2)
Crystal size (mm)	$0.04 \times 0.10 \times 0.10$	$0.10 \times 0.10 \times 0.60$
Crystal color	Yellow	Orange
Crystal habit	Prism	Prism
λ (Å)	0.71073	0.71073
μ (mm^{-1})	0.21	1.197
$2\theta_{max}$ (°)	74.7	69.4
Index ranges	$-9 \leqslant h \leqslant 7$; $-11 \leqslant k \leqslant 14$; $-20 \leqslant l \leqslant 21$	$-14 \leqslant h \leqslant 14$; $-30 \leqslant k \leqslant 30$; $-15 \leqslant l \leqslant 17$
Reflections collected/used in refinement	8742/5613	74670/7340
No. of refined parameters	243	243
R/R_w values	0.0646/0.1581	0.0776/0.2202
GOF on F^2	0.884	1.1
Final shift	0.000	0.000
$(\Delta\rho)_{min}$, $(\Delta\rho)_{max}$ (e Å^{-3})	0.288/−0.275	0.493/−0.329

Table 2. Selected bond lengths and angles (°, Å) for **3e** and **3f**

3e		**3f**	
C1–O1	1.396(3)	C1–O1	1.213(3)
C1–N1	1.313(3)	C1–N1	1.367(3)
C1–C2	1.612(4)	C1–C2	1.509(4)
C2–N3	1.163(3)	C2–N3	1.291(3)
C2–C3	1.575(4)	C2–C3	1.448(3)
C5–F1	1.567(4)	C5–F1	1.355(3)
C8–N1	1.630(4)	C8–N1	1.409(3)
C9–N2	1.253(3)	C9–N2	1.436(3)
C9–N1	1.478(3)	C9–N1	1.459(3)
C10–N2	1.423(3)	C10–N2	1.463(3)
C10–C11	1.302(4)	C10–C11	1.486(4)
C11–O2	1.481(4)	C11–C12	1.503(5)
C12–O2	1.357(4)	C12–C13	1.516(5)
C12–C13	1.311(4)	C13–C14	1.500(4)
C13–N2	1.532(4)	C14–N2	1.471(3)
C14–N4	1.245(3)	C15–N5	1.323(3)
C14–N5	1.451(4)	C15–N4	1.369(3)
C14–S1	1.864(3)	C15–S1	1.669(3)
C15–C16	1.645(5)	C16–C17	1.440(4)
C15–N5	1.327(3)	C16–N5	1.456(3)
C16–C17	1.238(5)	C17–C18	1.201(5)
N3–N4	1.492(3)	N3–N4	1.341(3)
C1–N1–C8	116.6(2)	C1–N1–C8	110.7(2)
C1–N1–C9	111.9(2)	C1–N1–C9	124.6(2)
C14–N4–N3	116.8(2)	N3–N4–C15	121.6(2)
C15–N5–C14	116.7(3)	C15–N5–C16	124.9(2)
N3–C2–C1	119.8(3)	N3–C2–C1	126.7(2)
N1–C9–N2–C10	160.0(2)	N1–C9–N2–C10	166.1(2)
N2–C9–N1–C1	118.3(3)	N2–C9–N1–C1	106.3(3)
C1–C2–N3–N4	−1.0(3)	C1–C2–N3–N4	−1.0(3)
S1–C14–N5–C15	1.1(4)	S1–C15–N5–C16	−1.4(4)

of C12. The shortest distances between the mentioned atoms and centroids of the benzene or pyrrole rings of indole range from 3.0 to 3.31 Å, with centroid angles ranging from 86.0 to 151.5°. In molecule **3f**, there are also two intermolecular C–H···π interactions between the pyrrole and either benzene rings of the indole heterocycle or C18 atom of allyl group of symmetry related molecule. The other C–H···π interaction is between C16 atom and the benzene ring of indole. The shortest distances between the mentioned atoms and centroids of benzene and pyrrole rings of indole range from 3.08 to 3.18 Å, with centroid angles ranging from 129.7° to 148.5°, both ranges being observed for classical C–H···π interactions.[24]

2.3. Primary antituberculosis activity

The new 5-fluoro-1*H*-indole-2,3-diones **2a**–**k** and **3a**–**r**, along with the previously synthesized[19,20] 5-nitro-1*H*-indole-2,3-dione-3-thiosemicarbazones **2l**–**v**, 1-morpholino/piperidinomethyl-5-nitro-1*H*-indole-2,3-dione-3-thiosemicarbazones **4a**–**l**, and 5-nitro-1*H*-indole-2,3-dione-3-[(4-oxo-1,3-thiazolidin-2-ylidene)hydrazones] **5a**–**s**, were evaluated at 6.25 μg/mL for in vitro anti-TB activity against *Mycobacterium tuberculosis* H37Rv (ATCC 27294) in BACTEC 12B medium using a broth microdilution assay, the Microplate Alamar Blue Assay (MABA). The fluorescence exhibiting compounds **2a**, **2f**, **2l**, **3h**, and **4a** were tested in the BACTEC 460 radiometric system in BACTEC 12B medium. The primary anti-TB screening was performed in accordance with the protocol of the

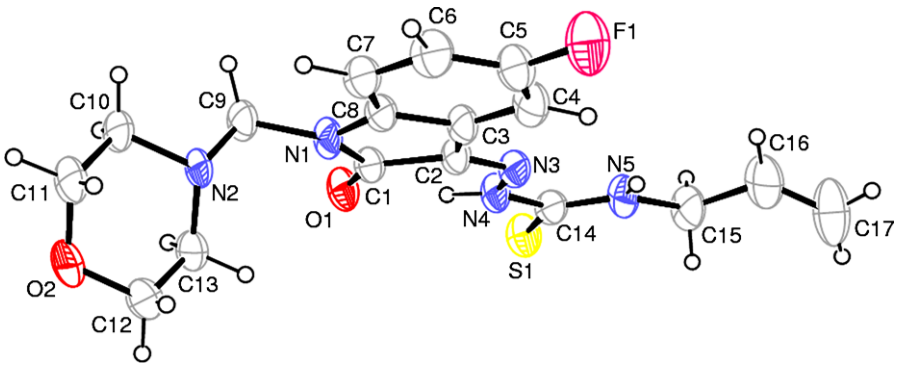

Figure 2. Molecular structure of **3e** showing the atom labeling scheme. Displacement ellipsoids are drawn as 30% probability level.

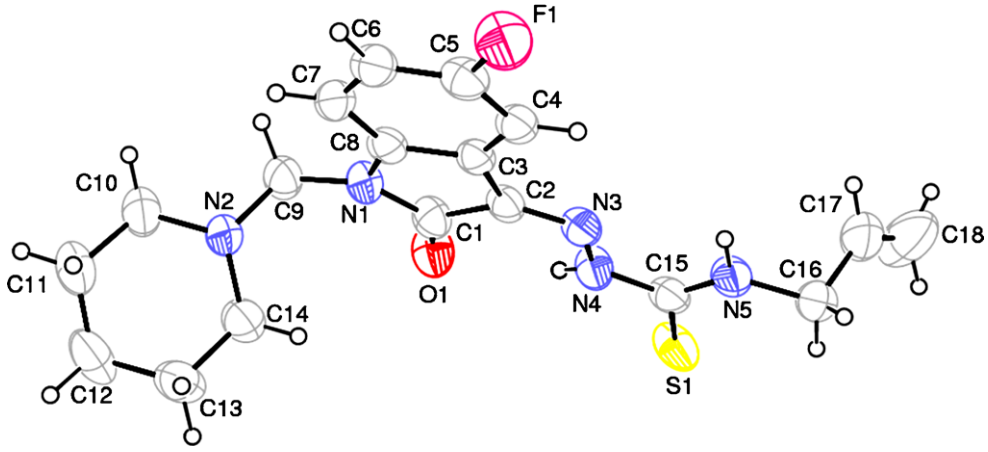

Figure 3. Molecular structure of **3f** showing the atom labeling scheme. Displacement ellipsoids are drawn as 30% probability level.

Table 3. Hydrogen bonding and short contact geometry for **3e** and **3f** (Å, °)

Compound	D–H···A	D–H	H···A	D···A	D–H···A
3e	N4–H4N···O1	0.98(3)	1.88(3)	2.610(3)	130(2)
	C4–H4···F1^{i}	0.93	2.43	3.355(4)	177
	C6-H6···O2^{ii}	0.93	2.32	2.932(4)	123
	C9-H9B···O1	0.97	2.27	2.778(3)	111
3f	N4–H4···O1	0.97(2)	1.92(2)	2.727(3)	139(2)
	N5–H5···N3	1.02(3)	2.28(3)	2.648(3)	100(2)
	N5–H5···S1^{iii}	1.02(3)	2.49(3)	3.433(2)	154(2)
	C16–H16B···S1	0.97	2.71	3.139(3)	107

Symmetry codes: (i) $2-x,1-y,1-z$; (ii) $3-x,1-y,-z$; (iii) $x,1/2-y,1/2+z$.

Tuberculosis Antimicrobial Acquisition and Coordinating Facility (TAACF) Southern Research Institute.[25] Rifampin was used as control drug in the tests. Activity of the compound was estimated as the percent inhibition (Table 4). Compounds demonstrating at least 90% inhibition in the primary screen were retested against *M. tuberculosis* H37Rv to determine the actual minimum inhibitory concentration (MIC) in the MABA. The MIC was defined as the lowest concentration effecting a reduction in fluorescence of 90% relative to controls. Concurrent with the determination of MICs, compounds were tested for cytotoxicity (IC_{50}) in VERO cells at concentrations 10× the MIC for *M. tuberculosis* H37Rv. However, as can be seen from Table 5, the whole of the tested compounds had high cytotoxicity.

When these data are examined, it is observed that in 1*H*-indole-2,3-dione-3-thiosemicarbazones and its N-Mannich bases, most of R^1-nitro substituted derivatives were more active than R^1-fluoro substituted derivatives. In fact, 5-nitro-1*H*-indole-2,3-dione-3-thiosemicarbazones (**2p**, **2r**, **2s**, and **2t**) and 1-morpholinomethyl-5-nitro-1*H*-indole-2,3-dione-3-thiosemicarbazones (**4a**, **4e**–**g**, **4i**, and **4j**) exhibited significant inhibitory activity (MIC $\geqslant$ 75%), whereas 5-fluoro-1*H*-indole-2,3-dione-3-thiosemicarbazones (**2e** and **2g**–**k**) and its N-Mannich bases (**3g**, **3i**, and **3l**–**r**) showed average activity

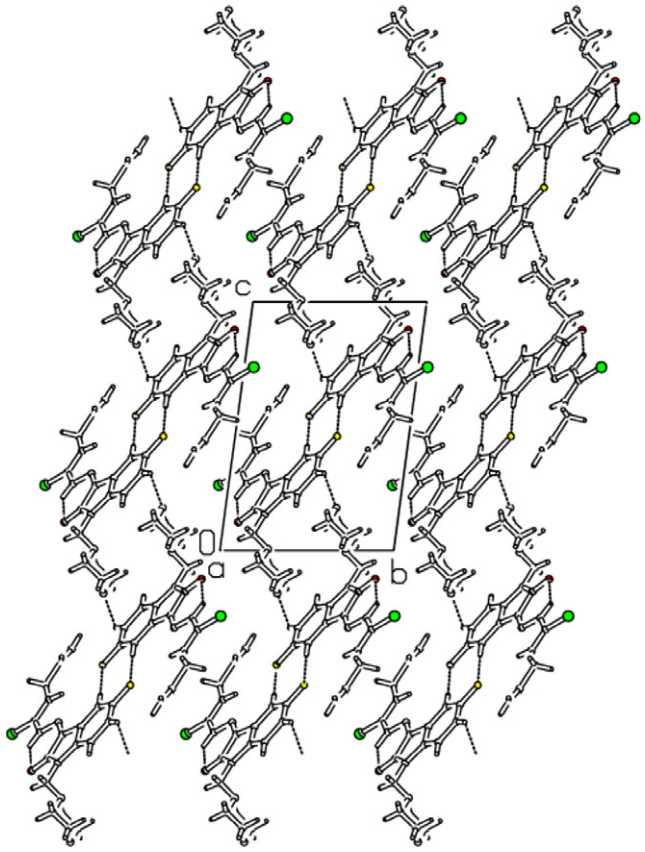

Figure 4. Crystal packing of **3e** showing the dimers and the dimer interactions. Dotted lines show the intermolecular interactions.

(31% ⩽ MIC ⩽ 70%). 5-Nitro-1*H*-indole-2,3-dione-3-thiosemicarbazones (**2p**, **2r**, and **2s**) and 1-morpholinomethyl-5-nitro-1*H*-indole-2,3-dione-3-thiosemicarbazones (**4a**, **4e**, **4g**, and **4i**), demonstrating at least 90% inhibition in the primary screen, are actually the most potent inhibitors of *M. tuberculosis* growth described in this study. While compounds **2r** and **4e** displayed anti-TB activity showing 93% and 90% inhibition, respectively, at a MIC value of 6.25 μg/mL, compounds **2p**, **2s**, **4a**, **4g**, and **4i** exhibited anti-TB activity showing 90%, 90%, 96%, 93%, and 92% inhibition, respectively, at a MIC value of >6.25 μg/mL.

Comparison of the thiosemicarbazones (**2a**–**v**), its N-Mannich bases (**3a**–**r** and **4a**–**l**) and thiazolidinones (**5a**–**s**) revealed that the anti-TB activity was increased due to elongation of the alkyl chain. Generally, replacement of the alkyl in the R_2 position with cyclohexyl or (non)substituted phenyl has been found to yield more active compounds (except for **4a**). Moreover, the 1-morpholinomethyl derivatives were more active than the corresponding the 1-piperidinomethyl derivatives. The presence of the morpholine ring in some R_1-nitro substituted N-Mannich bases also seems to have a significant impact on the resultant anti-TB activity. Compound **4a**, a morpholine derivative incorporating a methyl group at R_2, was found to be one of the most active inhibitors, whereas ligand **2l** was inactive. It is interesting to note that, for the R_2-phenyl substituted N-Mannich derivatives **4g** and **4h**, the morpholine derivative **4g** was substantially more active than both the ligand **2q** and the piperidine derivative **4h**, whereas the activity of **4h** was virtually unchanged when compared with the ligand **2q**. There were only minor variations in activities of other N-Mannich bases.

In comparison with compounds **2l**–**v**, none of the 4-thiazolidinone derivatives (**5**) were active against *M. tuberculosis*. These modifications of parent molecules led to a complete loss of the anti-TB activity. Further modifications of the structure of **2** may indeed lead to an improved antimycobacterial compound with more potency and less cytotoxicity.

Thus, the complex of pharmacophores and anti-pharmacophores, taken as a whole, plays an important role not only in the prediction of activities, but in the search for new drugs as well. The set of activity/inactivity

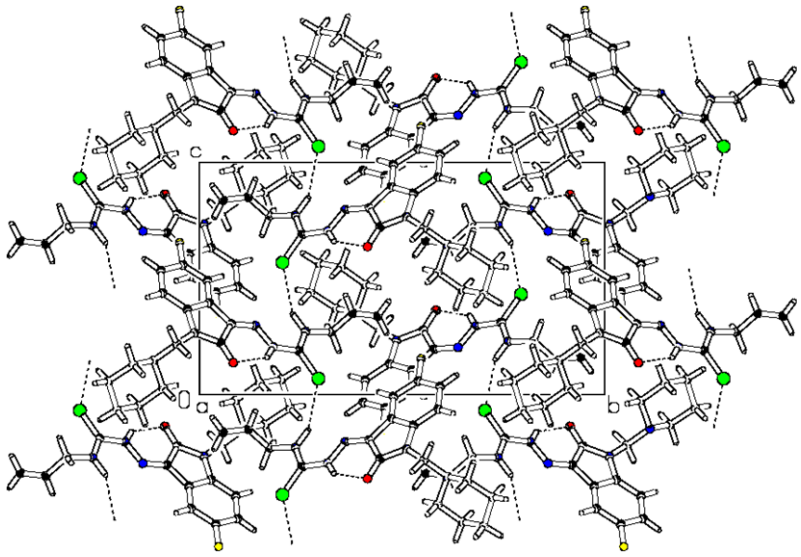

Figure 5. Crystal packing of **3f**. Dotted lines show the intermolecular interactions.

Table 4. Primary in vitro antituberculosis activity screening results of **2**–**5** against *M. tuberculosis* H37Rv at 6.25 μg/mL

Compound	R_1	R_2	R_3	X	GI (%)[a]	Compound	R_1	R_2	R_3	X	GI (%)[a]
2a	F	CH_3	—	—	0	**3o**	F	4-ClC_6H_4	—	O	58
2b	F	C_2H_5	—	—	8	**3p**	F	4-ClC_6H_4	—	CH_2	63
2c	F	CH_2–CH=CH_2	—	—	30	**3q**	F	4-FC_6H_4	—	O	48
2d	F	*n*-C_4H_9	—	—	16	**3r**	F	4-FC_6H_4	—	CH_2	38
2e	F	cycl-C_6H_{11}	—	—	39	**4a**	NO_2	CH_3	—	O	96
2f	F	$C_6H_5CH_2$	—	—	0	**4b**	NO_2	CH_2–CH=CH_2	—	O	19
2g	F	C_6H_5	—	—	61	**4c**	NO_2	CH_2–CH=CH_2	—	CH_2	22
2h	F	4-$CH_3C_6H_4$	—	—	36	**4d**	NO_2	*n*-C_4H_9	—	O	30
2i	F	4-ClC_6H_4	—	—	37	**4e**	NO_2	cycl-C_6H_{11}	—	O	90
2j	F	4-FC_6H_4	—	—	58	**4f**	NO_2	cycl-C_6H_{11}	—	CH_2	87
2k	F	4-$NO_2C_6H_4$	—	—	31	**4g**	NO_2	C_6H_5	—	O	93
2l	NO_2	CH_3	—	—	0	**4h**	NO_2	C_6H_5	—	CH_2	31
2m	NO_2	C_2H_5	—	—	0	**4i**	NO_2	4-$CH_3C_6H_4$	—	O	92
2n	NO_2	CH_2–CH=CH_2	—	—	25	**4j**	NO_2	4-$CH_3C_6H_4$	—	CH_2	88
2o	NO_2	*n*-C_4H_9	—	—	42	**4k**	NO_2	4-ClC_6H_4	—	O	65
2p	NO_2	cycl-C_6H_{11}	—	—	90	**4l**	NO_2	4-ClC_6H_4	—	CH_2	54
2q	NO_2	C_6H_5	—	—	33	**5a**	NO_2	CH_3	H	—	0
2r	NO_2	4-$CH_3C_6H_4$	—	—	93	**5b**	NO_2	C_2H_5	H	—	0
2s	NO_2	4-BrC_6H_4	—	—	90	**5c**	NO_2	CH_2–CH=CH_2	H	—	2
2t	NO_2	4-ClC_6H_4	—	—	75	**5d**	NO_2	*n*-C_4H_9	H	—	0
2u	NO_2	4-FC_6H_4	—	—	24	**5e**	NO_2	cycl-C_6H_{11}	H	—	0
2v	NO_2	4-$NO_2C_6H_4$	—	—	2	**5f**	NO_2	C_6H_5	H	—	0
3a	F	CH_3	—	O	12	**5g**	NO_2	4-$CH_3C_6H_4$	H	—	17
3b	F	CH_3	—	CH_2	20	**5h**	NO_2	4-BrC_6H_4	H	—	0
3c	F	C_2H_5	—	O	1	**5i**	NO_2	4-ClC_6H_4	H	—	0
3d	F	C_2H_5	—	CH_2	2	**5j**	NO_2	4-FC_6H_4	H	—	0
3e	F	CH_2–CH=CH_2	—	O	24	**5k**	NO_2	CH_2–CH=CH_2	CH_3	—	3
3f	F	CH_2–CH=CH_2	—	CH_2	20	**5l**	NO_2	*n*-C_4H_9	CH_3	—	10
3g	F	*n*-C_4H_9	—	O	34	**5m**	NO_2	cycl-C_6H_{11}	CH_3	—	28
3h	F	*n*-C_4H_9	—	CH_2	0	**5n**	NO_2	C_6H_5	CH_3	—	9
3i	F	cycl-C_6H_{11}	—	O	33	**5o**	NO_2	4-$CH_3C_6H_4$	CH_3	—	0
3j	F	$C_6H_5CH_2$	—	O	0	**5p**	NO_2	4-BrC_6H_4	CH_3	—	3
3k	F	$C_6H_5CH_2$	—	CH_2	3	**5q**	NO_2	4-ClC_6H_4	CH_3	—	0
3l	F	C_6H_5	—	O	56	**5r**	NO_2	4-FC_6H_4	CH_3	—	5
3m	F	C_6H_5	—	CH_2	45	**5s**	NO_2	4-$NO_2C_6H_4$	CH_3	—	9
3n	F	4-$CH_3C_6H_4$	—	CH_2	51						

[a] Growth inhibition of virulent H37Rv strain of *M. tuberculosis*.

Table 5. The GI, MIC, and IC_{50}values of **2p**, **2r**, **2s**, **4a**, **4e**, **4g**, and **4i** against *M. tuberculosis* H37Rv

Compound	GI[a] (%)	MIC[b] (μg/mL)	IC_{50}[c] (μg/mL)
2p	90	>6.25	4.74
2r	93	6.25	2.45
2s	90	>6.25	2.59
4a	96	>6.25	7.61
4e	90	6.25	[d]
4g	93	>6.25	2.8
4i	92	>6.25	17
Rifampin	97	0.125	>100

[a] Growth Inhibition of virulent H37Rv strain of *M. tuberculosis*.
[b] The actual minimum inhibitory concentration.
[c] The cytotoxicity.
[d] Insoluble in DMSO at 1 mg/mL. Unable to determine cytotoxicity.

fragments obtained in this study constitutes a basis for the development of a system for the anti-TB activity prediction.

2.4. Data sets

Compounds under study (71 in total, see Scheme) are shown along with their common structural skeletons in Table 4. A preliminary analysis of the molecules included optimization of their structures. Further the optimized structures were used in quantum-chemical calculations (AM1-method)[26] and their results provided various input data in the course of the ETM application. With the aim of more detailed SAR analysis, all compounds were separated into four groups. The first series included 10 compounds with high antituberculosis activity (MIC $\geqslant$ 75%). The second series contained 20 molecules with average activity (31% $\leqslant$ MIC $\leqslant$ 70%). The third and fourth sets of low-active (5% $\leqslant$ MIC $\leqslant$ 30%) and inactive compounds (MIC < 4%) included 19 and 22 molecules, respectively. The ETM has been applied to each set separately to identify the pharmacophores and anti-pharmacophores.

2.5. The search for pharmacophores (Ph) and anti-pharmacophores (APh) by using ETM

The ETM analyzes molecules represented by matrices which are named electronic-topological matrices of conjunction (ETMC), because they are formed of electronic and 3D-topology data.[27–30] Since details of the ETM can be found in literature,[31,32] we give here only the

most distinguished properties of the ETM relative to other methods used in SAR studies. When the system for the antituberculosis activity prognostication has been formed, compounds that represent each series and possess the highest levels of inhibitory activity and selectivity in the given group have been taken as templates to be compared with the rest of compounds as ETMCs.

From the ETM application to the series mentioned, a number of pharmacophores (Ph_i) have been calculated, which form the base of the system for the antituberculosis activity prognostication. Besides the pharmacophores, molecular fragments responsible for the activity loss (or anti-pharmacophores—APh_i) have been revealed as well. They are structural fragments that can be found in inactive compounds only. As an example, skeletons of template compounds and *submatrices* of their ETMCs (named as ETSCs, for short) are shown in Figures 6 and 7, which correspond to some of the pharmacophores and anti-pharmacophores.

As the first step, the compounds from the 1st and 4th groups were compared (i.e., high active and inactive ones). The ETM-calculations detected an activity feature 1 (named as a Ph1 pharmacophore), that is common for all high-active compounds. Ph1 and the corresponding ETSC ($ETSC_{Ph1}$) which has been calculated relative to the template compound **4a** are shown in Figure 6a. The $ETSC_{Ph1}$ is of the order 7×7, and only

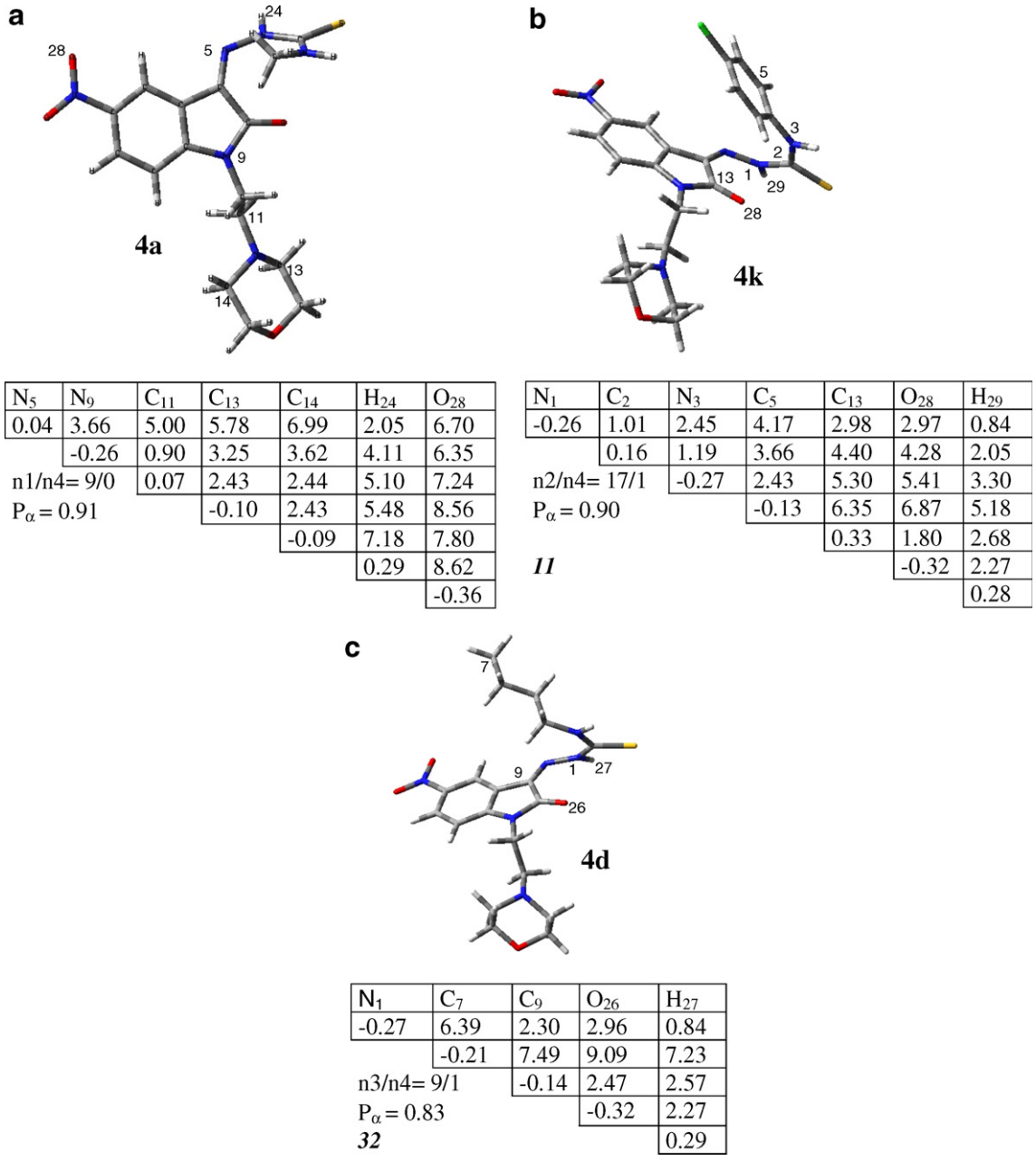

N_5	N_9	C_{11}	C_{13}	C_{14}	H_{24}	O_{28}
0.04	3.66	5.00	5.78	6.99	2.05	6.70
	-0.26	0.90	3.25	3.62	4.11	6.35
n1/n4= 9/0		0.07	2.43	2.44	5.10	7.24
$P_\alpha = 0.91$			-0.10	2.43	5.48	8.56
				-0.09	7.18	7.80
					0.29	8.62
						-0.36

N_1	C_2	N_3	C_5	C_{13}	O_{28}	H_{29}
-0.26	1.01	2.45	4.17	2.98	2.97	0.84
	0.16	1.19	3.66	4.40	4.28	2.05
n2/n4= 17/1		-0.27	2.43	5.30	5.41	3.30
$P_\alpha = 0.90$			-0.13	6.35	6.87	5.18
				0.33	1.80	2.68
11					-0.32	2.27
						0.28

N_1	C_7	C_9	O_{26}	H_{27}
-0.27	6.39	2.30	2.96	0.84
	-0.21	7.49	9.09	7.23
n3/n4= 9/1		-0.14	2.47	2.57
$P_\alpha = 0.83$			-0.32	2.27
32				0.29

Figure 6. Sub-matrices and corresponding structures of the Ph1–Ph3 pharmacophores, obtained relative to the template (active) compounds **4a**, **4k**, and **4d**.

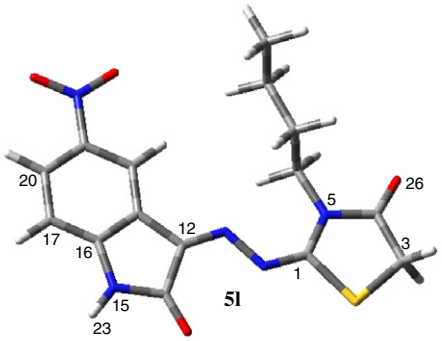

a

C_1	N_5	N_{15}	C_{16}	H_{23}	O_{26}
0.07	1.00	5.49	5.77	6.27	3.51
	-0.31	6.51	6.55	7.36	2.27
		-0.30	1.11	0.88	8.76
			0.14	2.05	8.76
n4/n1= 21/0				0.25	9.60
P_α = 0.96					-0.30

b

C_1	C_{12}	C_{16}	H_{23}	O_{26}
0.07	3.43	5.77	6.27	3.51
	-0.02	2.34	3.23	6.53
		0.14	2.05	8.76
n4/n2= 18/1			0.25	9.60
P_α = 0.90				-0.29

c

C_3	N_5	N_{15}	C_{17}	C_{20}
-0.35	2.40	8.00	9.66	10.01
	-0.31	6.51	7.74	7.90
		-0.30	2.51	3.72
n4/n3= 12/1			-0.20	1.44
P_α = 0.87				0.00

Figure 7. Sub-matrices and corresponding structures of the APh1–APh3 anti-pharmacophores, obtained relative to the template (inactive) compound **5l**.

its upper triangle is given because of the symmetry of bonds. There are two chemically bonded atoms N_9–C_{11} in Ph1, and the Wiberg's index (electronic population on bond) is given for this bond as the $W_{N9\text{–}C11}$ element of the submatrix ($W_{N9\text{–}C11}$ = 0.90). All other off-diagonal elements of the $ETSC_{Ph1}$ are 3D-distances for the corresponding pairs of atoms in the Ph1. This pharmacophore was found in 9 active compounds (n_1 = 9), while for inactive compounds it was not found (n_4 = 0). In this way, the probability P_α of the Ph1 presence in the set of high-active compounds was estimated as 0.91: P_α (Ph_i) = (n_1+1)/(n_1 + n_4+2), where n_1, n_4 are numbers of high active/inactive compounds, respectively, that contain the Ph. In the case of an anti-pharmacophore (APh_i), the corresponding probability P_{ia} is calculated in the same way, but (n_4 + 1) is to be used at place of (n_1 + 1) in the equation.

Seven atoms of the Ph1 pharmacophore belong to different parts of the template molecule. All these atoms have specific electronic-topological parameters (here, atomic charges and inter-atomic 3D-distances) that are contained in the $ETSC_{Ph1}$. As seen from Figure 6a, Ph1 includes properties of three main parts of active compounds that is indole, thiosemicarbazone, and morpholine.

Analogous ETSCs were obtained when compounds from other groups had been compared. Thus, the pharmacophore Ph2 (Fig. 6b) was found for the template **4k** from the comparison of compounds belonging to the 2nd and 4th groups. This pharmacophore is present in 17 active compounds (n_2 = 17) and one inactive compound (n_4 = 1). Thus, the probability of the Ph2 presence in the set of active compounds, P_α, was estimated as 0.90. Less informative pharmacophore was calculated from the comparison of the 3rd and 4th groups of compounds (Fig. 6c, template compound **4d**).

A 'break of activity', or antipharmacophore, was calculated relative to the inactive template compound **5l**. This antipharmacophore (APh1) was detected in 21 inactive compound (n_4 = 21) and was not found at all in the structures of high active compounds (n_1 = 0). The APh1 and its corresponding $ETSC_{APh1}$ calculated relative to the template compound **5l** are shown in Figure 7a.

The probability $P_i\alpha$ of the APh1 presence in the set of inactive compounds was estimated as 0.96. In Figures 7b and c, those antipharmacophores are shown that have been found from the 2nd and 3rd groups of compounds comparison.

2.6. Combined ETM–artificial neural networks approach (ETM–ANN)

The ETM data (initial matrices and the fragments found) can be used in the NN applications with the aim of obtaining the algorithmic base for the activity prediction. Here, some important observations as to their joint use are presented.

As known, Artificial Neural Networks (ANNs) can be divided into two main categories related to learning algorithms (i.e., supervised and unsupervised learning). First, the Kohonen neural network[33] (SOM, self-organized map) using an unsupervised learning algorithm has been applied to realize the projection of initial data (ETMCs) on the SOM units. Next, the supervised algorithm has been used for an feed forward neural network (FFNN) with backpropagation[34] to calculate dependencies between input and output variables being weights of the molecular fragments and activity values, correspondingly. The supervised learning was performed using a variant of FFNN known as the Associative Neural Network (ASNN).[35] Below, we briefly summarize the principles of this approach, while the detailed description of the algorithm can be found in the literature.[36]

It is clear that ETMCs cannot be used in a straightforward manner as the input for ANNs. Consequently, the information contained in ETMCs should be rear-

ranged somehow in order to serve as input vectors of equal dimensionality for an ANN. The training of the Kohonen's SOM has the property of mapping input vectors from the n-dimensional space ($n >> 2$), which possess similar properties to the same or nearby neurons in the two-dimensional space. Therefore, by considering all input vectors projected to the same output neuron, it is possible to determine clusters of vectors that have similar properties in the n-dimensional space.

In short, the principal idea of the combined approach is to determine the weights of fragments represented by ETSCs and, afterwards, to use these weights as *descriptors* (WDs) for the ASNNs training. To do this, the fragments are being projected on the Kohonen's maps that correspond to their initial ETMCs. In such way the degree of each fragment's presence in a molecule can be determined.

The first step is a procedure that can be called as 'triples calculation'. That is, data elements in the initial set are triples ($d1$, $d2$, $d3$), where $d1$ and $d2$ are charges for a pair of atoms and $d3$ is a connection between them. The values of di, $i = 1, 2, 3$, are taken from the ETMCs. The total number of triples equals to the amount of all two-atomic connections taken from all ETMCs. Second step is the Kohonen's network (SOM) initialization and training (detailed description of a Kohonen's network can be found in[37]). The approximate number of elements in our Kohonen's map is calculated as $S = k * S_{\mathrm{ETM}}$, where k varies in the range of, [1.0, 2.0] and S_{ETM} is the size of the largest ETM matrix. The third step involves the calculations of pharmacophores as submatrices of the template ETMCs. At the fourth step, the weight of each fragment (that is either a pharmacophore or antipharmacophore) is estimated versus each compound as the fragment's projection error, E_{ij}, relative to those nodes of the Kohonen's map that were found for its comprising ETMC. Then its weight is taken as the inverse of its error E_{ij}: $W_{ij} = 1 - E_{\mathrm{ij}}/E_{\mathrm{max},j}$. Here i is the molecule's number, j is the fragment's number, and $E_{\mathrm{max},j}$ is the maximal error, for all j. A new table containing the calculated fragment weights (descriptors) is being formed for further ASNN training.[35]

Briefly, the number of neurons in the input layer corresponds to the number of descriptors. The hidden layer contains five neurons. The bias neuron is presented both on the input and hidden layers. An ensemble of $M = 100$ neural networks was trained. By this, the activity values of each compound were calculated for each ASNN and averaged over all M networks. This value was used to calculate cross-validation coefficients.[38]

The quality of each final model was assessed by the leave-one-out method (LOO). By the method, each molecule is removed from the training set, and the remaining set is used to separate molecules into classes of activity, thereby predicting the activity of this molecule and evaluating the quality of the decision rule.

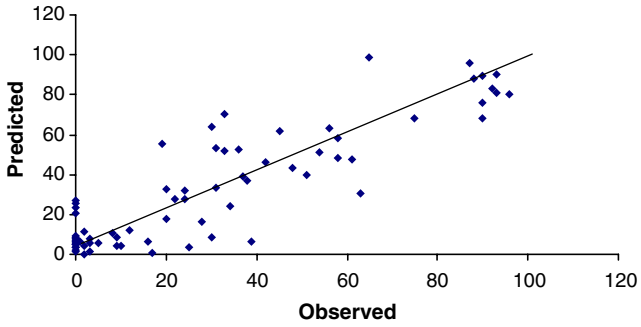

Figure 8. Plot of predicted antituberculosis activity versus actual observed values.

The last step includes application of the pruning methods[39,40] that aim in a set of the most relevant ETMC fragments selection.

2.7. ETM–ANN approach application

To reflect the realistic internal structure of the data, all compounds were separated into two main series. The first one included 49 active compounds, and the second series included 22 inactive compounds. For the data, 339 fragments were selected. The first step consisted of using the LOO cross-validation procedure for total set of compound. The ASNNs recognized correctly 88.7%, or 63 from 71 compounds. Next, the importance of the detected fragments for the observed activity was evaluated by using pruning methods. The most part of the ETMC fragments (as descriptors) were detected as non-significant and removed by the pruning algorithms. As the result, only 9 ETMC-fragments were chosen from 339 fragments in total as the most important ones. By this, ASNN classified correctly 94.4%, or 67 compounds from 71.

The main goal of the second stage in the data analysis was to evaluate an efficacy of ASNN in the SAR model generation for the real values of the activity. The first step was the LOO cross-validation procedure applied to the total set of compounds. It has been found that a cross-validated q^2 coefficient of the ASNN predictions was 0.68 ± 0.01. After applying the pruning methods 8 fragments were selected from 339 in total. The cross-validated q^2 value was 0.77 ± 0.01.

Thus, the obtained results indicate that application of pruning methods provides higher prognosing ability compared to the case when all descriptors are used for the activity prediction. As it is seen, the approach presented in this study has shown quite satisfactory results (Fig. 8). This fact tells in favor of workability of the both models found. These models can be applied to the design of new potent antituberculosis drugs.

3. Conclusions

A new series of 5-fluoro-1*H*-indole-2,3-dione-3-thiosemicarbazones and 5-fluoro-1-morpholino/piperidinomethyl-1*H*-indole-2,3-dione-3-thiosemicarbazones was

synthesized. The structures of the synthesized compounds were confirmed by spectral data, elemental and single crystal X-ray diffraction analysis. These new 5-fluoroindol-2,3-dione derivatives and 5-nitro-1*H*-indole-2,3-dione-3-thiosemicarbazones, as well as previously synthesized 1-morpholino/piperidinomethyl-5-nitro-1*H*-indole-2,3-dione-3-thiosemicarbazones and 5-nitro-1*H*-indole-2,3-dione-3-[(4-oxo-1,3-thiazolidin-2-ylidene)hydrazones], have been evaluated for the anti-TB activity. Among the tested compounds, 5-nitro-1*H*-indole-2,3-dione-3-thiosemicarbazones and 1-morpholinomethyl-5-nitro-1*H*-indole-2,3-dione-3-thiosemicarbazones showed good inhibitory activity in the primary screen. The anti-TB activity of molecules with diverse skeletons was investigated by means of the ETM. The structural fragments of activity and 'breaks of activity', as well as their numerical parameters found by the ETM, provide some rules, which are to be obeyed by active compounds. The more important is that these conditions can be directly used to design new active compounds with required properties.

All activity features detected by the ETM are characterized by the probabilities P_α that lie in the limits of 0.84–0.91. Comparison of the activity features with the 'breaks of activity' provides a detailed explanation of why the activity varies so much in all four series investigated.

4. Experimental

Melting points were estimated with a Buchi 540 melting point apparatus in open capillaries and are uncorrected. Elemental analyses were performed on a Thermo Finnigan Flash EA 1112 elemental analyzer. IR spectra were recorded on KBr disks, using a Perkin-Elmer Model 1600 FT-IR spectrometer. ^{1}H NMR, ^{13}C NMR APT, and HETCOR-2D spectra were obtained on Bruker Avance DPX 400 and Varian^{UNITY} INOVA 500 spectrophotometers using DMSO-d_6. Mass spectra were determined on Finnigan TM LCQ (Advantage Max LC/MS) or Mass-AILENT 1100 MSD instruments. All chemicals and solvents were purchased from Merck-Schuchardt, Aldrich, and Fluka.

4.1. General method for the synthesis of N-substituted thiosemicarbazides

To a solution of hydrazine hydrate (5 mmol) in ethanol, a suspension of an appropriate isothiocyanate (5 mmol) in ethanol was added dropwise with vigorous stirring and cooling in an ice bath. The mixture was allowed to stand overnight. The crystals formed were recrystallized from ethanol.

4.2. General method for the synthesis of 5-fluoro/nitro-1*H*-indole-2,3-dione-3-thiosemicarbazones (2a–v)[19]

A solution of N-substituted thiosemicarbazides (3.5 mmol) in ethanol (10 mL) was added to a solution of 5-fluoro/nitro-1*H*-indole-2,3-dione **1a/1b** (3.5 mmol) in ethanol (20 mL). After addition of a drop of concentrated sulfuric acid, the mixture was refluxed on a water bath for 5 h. The product formed after cooling was filtered and washed with ethanol or recrystallized from ethanol.

4.2.1. 5-Fluoro-1*H*-indole-2,3-dione-3-(*N*-methylthiosemicarbazone) (2a). Orange crystals (97%): mp 273–274 °C; IR (KBr): υ 3251 (NH), 1692 (C=O), 1148 (C=S); ^{1}H NMR (DMSO-d_6/400 MHz): δ 3.08 (d, J = 4.58 Hz, 3H, CH_3), 6.92 (dd, J = 8.58, 4.18 Hz, 1H, indole C_7–H), 7.18 (dt, J = 8.97, 2.97 Hz, 1H, indole C_6–H), 7.44 (dd, J = 8.13, 2.67 Hz, 1H, indole C_4–H), 9.32 (q, J = 4.56 Hz, 1H, N_4–H), 11.21 (s, 1H, indole NH), 12.47 (s, 1H, N_2–H); Anal. Calcd for $C_{10}H_9FN_4OS$ (252.26): C, 47.61; H, 3.60; N, 22.21. Found: C, 47.77; H, 3.25; N, 22.14.

4.2.2. 5-Fluoro-1*H*-indole-2,3-dione-3-(*N*-ethylthiosemicarbazone) (2b). Dark yellow crystals (92%): mp 245–246 °C; IR (KBr): υ 3325, 3173 (NH), 1687 (C=O), 1144 (C=S); ^{1}H NMR (DMSO-d_6/500 MHz): δ 1.21 (t, J = 7.17 Hz, 3H, ethyl CH_3), 3.66 (p, J = 6.56 Hz, 2H, ethyl CH_2), 6.93 (dd, J = 8.70, 4.12 Hz, 1H, indole C_7–H), 7.19 (dt, J = 8.54, 2.74 Hz, 1H, indole C_6–H), 7.50 (dd, J = 8.08, 2.59 Hz, 1H, indole C_4–H), 9.33 (t, J = 5.64 Hz, 1H, N_4–H), 11.20 (s, 1H, indole NH), 12.45 (s, 1H, N_2–H); ^{13}C NMR (HETCOR DMSO-d_6/100 MHz): δ 14.43 (ethyl CH_3), 39.33–40.58 (m, ethyl CH_2, DMSO), 108.17 (d, J = 25.8 Hz, indole C_4), 112.50 (d, J = 8.10 Hz, indole C_7), 117.71 (d, J = 24.1 Hz, indole C_6), 121.86 (d, J = 9.20 Hz, indole C_{3a}), 131.41 (d, J = 3.10 Hz, indole C_{7a}), 138.90 (indole C_3), 158.68 (d, J = 237.7 Hz, indole C_5), 163.13 (indole C=O), 177.11 (C=S); LCMS-APCI (−/+): m/z (%) 265 (MH^-, 100). Anal. Calcd for $C_{11}H_{11}FN_4OS$ (266.29): C, 49.61; H, 4.16; N, 21.04. Found: C, 49.41; H, 3.88; N, 21.19.

4.2.3. 5-Fluoro-1*H*-indole-2,3-dione-3-(*N*-allylthiosemicarbazone) (2c). Shining dark yellow crystals (74%): mp 219–220 °C; IR (KBr): υ 3371, 3175 (NH), 1691 (C=O), 1152 (C=S); ^{1}H NMR (DMSO-d_6/400 MHz): δ 4.27 (t, J = 5.38 Hz, 2H, allyl C_1–H_2), 5.16 (d, J = 10.28 Hz, 1H, allyl C_3–H_{cis}), 5.21 (d, J: 17.20 Hz, 1H, allyl C_3–H_{trans}), 5.89–5.96 (m, 1H, allyl C_2–H), 6.93 (dd, J = 8.55, 4.10 Hz, 1H, indole C_7–H), 7.19 (dt, J = 8.91, 2.59 Hz, 1H, indole C_6–H), 7.51 (dd, J = 8.14, 2.57 Hz, 1H, indole C_4–H), 9.52 (t, J = 5.79 Hz, 1H, N_4–H), 11.22 (s, 1H, indole NH), 12.50 (s, 1H, N_2–H); Anal. Calcd for $C_{12}H_{11}FN_4OS$ (278.30): C, 51.79; H, 3.98; N, 20.13. Found: C, 51.64; H, 3.61; N, 20.25.

4.2.4. 5-Fluoro-1*H*-indole-2,3-dione-3-(*N*-*n*-butylthiosemicarbazone) (2d). Yellow powder (81%): mp 211–212 °C; IR (KBr): υ 3246 (NH), 1694 (C=O), 1140 (C=S); ^{1}H NMR (DMSO-d_6/500 MHz): δ 0.93 (t, J = 7.32 Hz, 3H, butyl CH_3), 1.33–1.37 (m, 2H, butyl C_3–H_2), 1.63 (p, J = 7.39 Hz, 2H, butyl C_2–H_2), 3.62 (q, J = 6.91 Hz, 2H, butyl C_1–H_2), 6.92 (dd, J = 8.54, 4.27 Hz, 1H, indole C_7–H), 7.19 (dt, J = 8.42, 2.75 Hz, 1H, indole C_6–H), 7.51 (dd, J = 8.08, 2.59 Hz, 1H, indole C_4–H), 9.30 (t, J = 5.79 Hz, 1H, N_4–H), 11.19 (s, 1H, indole NH), 12.45 (s, 1H, N_2–H); ^{13}C NMR (APT

DMSO-d_6/100 MHz): δ 14.20 (butyl CH_3), 20.06 (butyl C_3), 30.96 (butyl C_2), 44.37 (butyl C_1), 108.21 (d, J = 25.7 Hz, indole C_4), 112.48 (d, J = 8.09 Hz, indole C_7), 117.69 (d, J = 24.1 Hz, indole C_6), 121.86 (d, J = 9.26 Hz, indole C_{3a}), 131.37 (d, J = 3.09 Hz, indole C_{7a}), 138.87 (indole C_3), 158.68 (d, J = 237.6 Hz, indole C_5), 163.13 (indole C=O), 177.31 (C=S); LCMS-APCI (−/+): m/z (%) 293 (MH^-, 100). Anal. Calcd for $C_{13}H_{15}FN_4OS$ (294.34): C, 53.05; H, 5.14; N, 19.03. Found: C, 52.97; H, 5.01; N, 19.02.

4.2.5. 5-Fluoro-1*H*-indole-2,3-dione-3-(*N*-cyclohexylthiosemicarbazone) (2e). Shining yellow crystals (89%): mp 249–250 °C; IR (KBr): υ 3360, 3171 (NH), 1692 (C=O), 1130 (C=S); ^{1}H NMR (DMSO-d_6/400 MHz): δ 1.15 (t, J = 12.54 Hz, 1H, cycl. C_4–H_{ax}), 1.28–1.35 (m, 2H, cycl. C_3–H_{ax}, C_5–H_{ax}), 1.42–1.51 (m, 2H, cycl. C_2–H_{ax}, C_6–H_{ax}), 1.64 (d, J = 12.14 Hz, 1H, cycl. C_4–H_{equiv}), 1.77 (d, J = 12.83 Hz, 2H, cycl. C_3–H_{equiv}, C_5–H_{equiv}), 1.92 (d, J = 9.78 Hz, 2H, cycl. C_2–H_{equiv}, C_6–H_{equiv}), 4.18–4.21 (m, 1H, cycl C_1–H), 6.92 (dd, J = 8.55, 4.17 Hz, 1H, indole C_7–H), 7.19 (dt, J = 9.08, 2.73 Hz, 1H, indole C_6–H), 7.62 (dd, J = 8.19, 2.71 Hz, 1H, indole C_4–H), 8.87 (d, J = 8.49 Hz, 1H, N_4–H), 11.21 (s, 1H, indole NH), 12.47 (s, 1H, N_2–H); ^{13}C NMR (HETCOR DMSO-d_6/100 MHz): δ 25.36 (cycl. C_3, C_5), 25.57 (cycl. C_4), 31.96 (cycl. C_2, C_6), 54.27 (cycl. C_1), 108.60 (d, J = 25.7 Hz, indole C_4), 112.46 (d, J = 8.10 Hz, indole C_7), 117.76 (d, J = 24.1 Hz, indole C_6), 121.83 (d, J = 9.41 Hz, indole C_{3a}), 131.57 (d, J = 3.23 Hz, indole C_{7a}), 138.91 (indole C_3), 158.70 (d, J = 237.4 Hz, indole C_5), 163.17 (indole C=O), 176.17 (C=S). Anal. Calcd for $C_{15}H_{17}FN_4OS$ (320.38): C, 56.23; H, 5.35; N, 17.49. Found: C, 55.96; H, 4.81; N, 17.52.

4.2.6. 5-Fluoro-1*H*-indole-2,3-dione-3-(*N*-benzylthiosemicarbazone) (2f). Shining orange crystals (92%): mp 246–247 °C; IR (KBr): υ 3312, 3207 (NH), 1690 (C=O), 1140 (C=S); ^{1}H NMR (DMSO-d_6/500 MHz): δ 4.90 (d, J = 6.41 Hz, 2H, benzyl CH_2), 6.93 (dd, J = 8.54, 4.27 Hz, 1H, indole C_7–H), 7.20 (dt, J = 9.15, 2.75 Hz, 1H, indole C_6–H), 7.28 (t, J = 6.86 Hz, 1H, benzyl C_4–H), 7.34–7.39 (m, 4H, benzyl C_2–H, C_3–H, C_5–H, C_6–H), 7.49 (dd, J = 8.24, 2.74 Hz, 1H, indole C_4–H), 9.87 (t, J = 6.10 Hz, 1H, N_4–H), 11.24 (s, 1H, indole NH), 12.57 (s, 1H, N_2–H); LCMS-APCI (−/+): m/z (%) 327 (MH^-, 100). Anal. Calcd for $C_{16}H_{13}FN_4OS$ (328.36): C, 58.52; H, 3.99; N, 17.06. Found: C, 58.52; H, 3.77; N, 17.23.

4.2.7. 5-Fluoro-1*H*-indole-2,3-dione-3-(*N*-phenylthiosemicarbazone) (2g). Orange powder (79%): mp 218 °C; IR (KBr): υ 3363, 3177 (NH), 1690 (C=O), 1142 (C=S); ^{1}H NMR (DMSO-d_6/400 MHz): δ 6.93 (dd, J = 8.56, 4.17 Hz, 1H, indole C_7–H), 7.20 (dt, J = 8.37, 2.72 Hz, 1H, indole C_6–H), 7.29 (t, J = 7.16 Hz, 1H, phenyl C_4–H), 7.44 (t, J = 7.01 Hz, 2H, phenyl C_3–H, C_5–H), 7.62 (d, J = 7.44 Hz, 2H, phenyl C_2–H, C_6–H), 7.65 (dd, J = 8.02, 2.68 Hz, 1H, indole C_4–H), 10.81 (s, 1H, N_4–H), 11.22 (s, 1H, indole NH), 12.67 (s, 1H, N_2–H); LCMS-APCI (−/+): m/z (%) 313 (MH^-, 12), 178 (100), 315 (MH^+, 72), 180 (100). Anal. Calcd for $C_{15}H_{11}FN_4OS$ (314.33): C, 57.31; H, 3.53; N, 17.82. Found: C, 57.19; H, 3.16; N, 17.73.

4.2.8. 5-Fluoro-1*H*-indole-2,3-dione-3-[*N*-(4-methylphenyl)-thiosemicarbazone] (2h). Orange powder (89%): mp 244–246 °C; IR (KBr): υ 3315, 3242 (NH), 1692 (C=O), 1133 (C=S). ^{1}H NMR (DMSO-d_6/400 MHz): δ 2.17 (s, 3H, CH_3), 6.78 (dd, J = 8.55, 4.16 Hz, 1H, indole C_7–H), 7.04 (dt, J = 9.30, 2.64 Hz, 1H, indole C_6–H), 7.08 (d, J = 8.34 Hz, 2H, phenyl C_3–H, C_5–H), 7.31 (d, J = 8.25 Hz, 2H, phenyl C_2–H, C_6–H), 7.48 (dd, J = 8.15, 2.56 Hz, 1H, indole C_4–H), 10.63 (s, 1H, N_4–H), 11.09 (s, 1H, indole NH), 12.49 (s, 1H, N_2–H); LCMS-APCI (−/+): m/z (%) 329 (MH^+, 39), 180 (97), 152 (100). Anal. Calcd for $C_{16}H_{13}FN_4OS$ (328.36): C, 58.52; H, 3.99; N, 17.06. Found: C, 58.69; H, 4.02; N, 17.04.

4.2.9. 5-Fluoro-1*H*-indole-2,3-dione-3-[*N*-(4-chlorophenyl)-thiosemicarbazone] (2i). Orange powder (97%): mp 260 °C; IR (KBr): υ 3319, 3195 (NH), 1689 (C=O), 1149 (C=S); ^{1}H NMR (DMSO-d_6/400 MHz): δ 6.78 (dd, J = 8.56, 4.16 Hz, 1H, indole C_7–H), 7.05 (dt, J = 9.05, 2.70 Hz, 1H, indole C_6–H), 7.34 (d, J = 8.75 Hz, 2H, phenyl C_3–H, C_5–H), 7.45 (dd, J = 8.13, 2.65 Hz, 1H, indole C_4–H), 7.51 (d, J = 8.76 Hz, 2H, phenyl C_2–H, C_6–H), 10.72 (s, 1H, N_4–H), 11.11 (s, 1H, indole NH), 12.51 (s, 1H, N_2–H). Anal. Calcd for $C_{15}H_{10}ClFN_4OS$ (348.78): C, 51.65; H, 2.89; N, 16.06. Found: C, 52.13; H, 2.74; N, 16.06.

4.2.10. 5-Fluoro-1*H*-indole-2,3-dione-3-[*N*-(4-fluorophenyl)-thiosemicarbazone] (2j). Orange powder (89%): mp 246–248 °C; IR (KBr): υ 3331, 3194 (NH), 1692 (C=O), 1146 (C=S); ^{1}H NMR (DMSO-d_6/400 MHz): δ 6.78 (dd, J = 8.56, 4.15 Hz, 1H, indole C_7–H), 7.03 (dt, J = 8.76, 2.52 Hz, 1H, indole C_6–H), 7.12 (t, J = 8.79 Hz, 2H, phenyl C_3–H, C_5–H), 7.43–7.46 (m, 3H, indole C_4–H, phenyl C_2–H, C_6–H), 10.63 (s, 1H, N_4–H), 11.10 (s, 1H, indole NH), 12.52 (s, 1H, N_2–H); LCMS-APCI (−/+): m/z (%) 331 (MH^-, 21), 178 (100), 333 (MH^+, 82), 180 (100). Anal. Calcd for $C_{15}H_{10}F_2N_4OS$ (332.32): C, 54.21; H, 3.03; N, 16.86. Found: C, 53.84; H, 3.00; N, 16.82.

4.2.11. 5-Fluoro-1*H*-indole-2,3-dione-3-[*N*-(4-nitrophenyl)-thiosemicarbazone] (2k). Orange powder (91%): mp 267 °C; IR (KBr): υ 3298, 3190 (NH), 1694 (C=O), 1154 (C=S); ^{1}H NMR (DMSO-d_6/500 MHz): δ 6.95 (dd, J = 8.54, 4.14 Hz, 1H, indole C_7–H), 7.24 (dt, J = 9.02, 2.28 Hz, 1H, indole C_6–H), 7.63 (dd, J = 7.81, 2.44 Hz, 1H, indole C_4–H), 8.09 (d, J = 9.27 Hz, 2H, phenyl C_2–H, C_6–H), 8.31 (d, J = 8.78 Hz, 2H, phenyl C_3–H, C_5–H), 11.09 (s, 1H, N_4–H), 11.30 (s, 1H, indole NH), 12.89 (s, 1H, N_2–H). Anal. Calcd for $C_{15}H_{10}FN_5O_3S$ (359.33): C, 50.14; H, 2.81; N, 19.49. Found: C, 49.81; H, 2.36; N, 19.88.

4.3. General method for the synthesis of 5-fluoro-1-morpholino/piperidinomethyl-1*H*-indole-2,3-dione-3-thiosemicarbazones (3a–r)

To a suspension of **2a**–**k** (2 mmol) in absolute ethanol (20 mL), 37% formaldehyde solution (0.5 mL) and

morpholine or piperidine (2 mmol) were added dropwise with vigorous stirring. After combining all reagents, the reaction mixture was stirred at room temperature for 10 h. The solid product was filtered and washed with petroleum ether.

4.3.1. 5-Fluoro-1-(morpholin-4-ylmethyl)-1*H*-indole-2,3-dione-3-(*N*-methylthiosemicarbazone) (3a). Yellow powder (98%): mp 209 °C; IR (KBr): υ 3239 (NH), 1694 (C=O), 1139 (C=S); ^{1}H NMR (DMSO-d_6, 400 MHz): δ 2.55 (t, J = 4.19 Hz, 4H, morph. C_3–H_2, C_5–H_2), 3.10 (d, J = 4.40 Hz, 3H, CH_3), 3.54 (t, J = 4.34 Hz, 4H, morph. C_2–H_2, C_6–H_2), 4.49 (s, 2H, N–CH_2–N), 7.28–7.30 (m, 2H, indole C_7–H, C_6–H), 7.51 (dd, J = 6.99, 2.13 Hz, 1H, indole C_4–H), 9.38 (br s, 1H, N_4–H), 12.39 (s, 1H, N_2–H). Anal. Calcd for $C_{15}H_{18}FN_5O_2S$ (351.39): C, 51.27; H, 5.16; N, 19.93. Found: C, 51.14; H, 5.31; N, 19.78.

4.3.2. 5-Fluoro-1-(piperidin-1-ylmethyl)-1*H*-indole-2,3-dione-3-(*N*-methylthiosemicarbazone) (3b). Yellow powder (85%): mp 186–187 °C; IR (KBr): υ 3242 (NH), 1695 (C=O), 1155 (C=S); ^{1}H NMR (DMSO-d_6/400 MHz): δ 1.33 (br s, 2H, pip. C_4–H_2), 1.45 (br s, 4H, pip. C_3–H_2, C_5–H_2), 2.51 (s, pip. C_2–H_2, C_6–H_2, DMSO), 3.09 (d, J = 4.52 Hz, 3H, CH_3), 4.46 (s, 2H, N–CH_2–N), 7.25–7.27 (m, 2H, indole C_7–H, C_6–H), 7.49 (dd, J = 7.98, 1.16 Hz, 1H, indole C_4–H), 9.36 (br s, 1H, N_4–H), 12.40 (s, 1H, N_2–H). Anal. Calcd for $C_{16}H_{20}FN_5OS$ (349.42): C, 55.00; H, 5.77; N, 20.04. Found: C, 54.42; H, 5.88; N, 20.04.

4.3.3. 5-Fluoro-1-(morpholin-4-ylmethyl)-1*H*-indole-2,3-dione-3-(*N*-ethylthiosemicarbazone) (3c). Yellow powder (97%): mp 184 °C; IR (KBr): υ 3279 (NH), 1698 (C=O), 1139 (C=S); ^{1}H NMR (DMSO-d_6, 500 MHz): δ 1.21 (t, J = 7.17 Hz, 3H, ethyl CH_3), 2.56 (t, J = 3.66 Hz, 4H, morph. C_3–H_2, C_5–H_2), 3.55 (t, J = 4.27 Hz, 4H, morph. C_2–H_2, C_6–H_2), 3.66 (p, J = 6.56 Hz, 2H, ethyl CH_2), 4.49 (s, 2H, N–CH_2–N), 7.27–7.29 (m, 2H, indole C_7–H, C_6–H), 7.55 (dd, J = 8.54, 1.52 Hz, 1H, indole C_4–H), 9.39 (t, J = 5.79 Hz, 1H, N_4–H), 12.36 (s, 1H, N_2–H); ^{13}C NMR (HETCOR DMSO-d_6/100 MHz): δ 14.42 (ethyl CH_3), 39.32–40.57 (m, ethyl CH_2, DMSO), 50.96 (morph. C_3, C_5), 61.81 (N–CH_2–N), 66.44 (morph. C_2, C_6), 107.78 (d, J = 26.0 Hz, indole C_4), 112.81 (d, J = 8.01 Hz, indole C_7), 117.50 (d, J = 24.0 Hz, indole C_6), 121.28 (d, J = 9.44 Hz, indole C_{3a}), 130.30 (d, J = 3.43 Hz, indole C_{7a}), 140.07 (d, J = 1.19 Hz, indole C_3), 159.12 (d, J = 238.36 Hz, indole C_5), 162.07 (indole C=O), 177.06 (C=S). Anal. Calcd for $C_{16}H_{20}FN_5O_2S$ (365.42): C, 52.59; H, 5.52; N, 19.16. Found: C, 52.52; H, 5.40; N, 19.16.

4.3.4. 5-Fluoro-1-(piperidin-1-ylmethyl)-1*H*-indole-2,3-dione-3-(*N*-ethylthiosemicarbazone) (3d). Orange powder (92%): mp 176–177 °C; IR (KBr): υ 3251 (NH), 1690 (C=O), 1142 (C=S); ^{1}H NMR (DMSO-d_6/500 MHz): δ 1.21 (t, J = 7.17 Hz, 3H, ethyl CH_3), 1.34 (br s, 2H, pip. C_4–H_2), 1.47 (p, J = 5.34 Hz, 4H, pip. C_3–H_2, C_5–H_2), 2.50–2.52 (m, DMSO, pip. C_2–H_2, C_6–H_2), 3.66 (p, J = 6.56 Hz, 2H, ethyl CH_2), 4.48 (s, 2H, N–CH_2–N), 7.27–7.28 (m, 2H, indole C_7–H, C_6–H), 7.55 (dd, J = 7.62, 1.83 Hz, 1H, indole C_4–H), 9.38 (t, J = 5.64 Hz, 1H, N_4–H), 12.38 (s, 1H, N_2–H); ^{13}C NMR (HETCOR DMSO-d_6/100 MHz): δ 14.41 (ethyl CH_3), 24.01 (pip. C_4), 25.81 (pip. C_3, C_5), 39.36–40.61 (m, pip. C_2, C_6, DMSO), 51.78 (ethyl CH_2), 62.51 (N–CH_2–N), 107.81 (d, J = 25.7 Hz, indole C_4), 112.85 (d, J = 7.96 Hz, indole C_7), 117.48 (d, J = 24.1 Hz, indole C_6), 121.20 (d, J = 9.38 Hz, indole C_{3a}), 130.25 (d, J = 3.22 Hz, indole C_{7a}), 140.34 (indole C_3), 159.05 (d, J = 238.48 Hz, indole C_5), 162.07 (indole C=O), 177.07 (C=S). Anal. Calcd for $C_{17}H_{22}FN_5OS$ (363.45): C, 56.18; H, 6.10; N, 19.27. Found: C, 55.95; H, 6.40; N, 19.01.

4.3.5. 5-Fluoro-1-(morpholin-4-ylmethyl)-1*H*-indole-2,3-dione-3-(*N*-allylthiosemicarbazone) (3e). Dark yellow powder (81%): mp 153–154 °C; IR (KBr): υ 3235 (NH), 1686 (C=O), 1155 (C=S); ^{1}H NMR (DMSO-d_6/400 MHz): δ 2.55 (t, J = 3.97 Hz, 4H, morph. C_3–H_2, C_5–H_2), 3.54 (t, J = 4.29 Hz, 4H, morph. C_2–H_2, C_6–H_2), 4.27 (t, J = 5.54 Hz, 2H, allyl C_1–H_2), 4.49 (s, 2H, N–CH_2–N), 5.16 (dd, J = 10.23, 1.53 Hz, 1H, allyl C_3–H_{cis}), 5.21 (dd, J = 17.24, 1.58 Hz, 1H, allyl C_3–H_{trans}), 5.89–5.96 (m, 1H, allyl C_2–H), 7.28–7.30 (m, 2H, indole C_7–H, C_6–H), 7.58 (dd, J = 7.72, 2.16 Hz, 1H, indole C_4–H), 9.58 (t, J = 5.86 Hz, 1H, N_4–H), 12.41 (s, 1H, N_2–H). Anal. Calcd for $C_{17}H_{20}FN_5O_2S$ (377.43): C, 54.10; H, 5.34; N, 18.56. Found: C, 54.10; H, 4.98; N, 18.65.

4.3.6. 5-Fluoro-1-(piperidin-1-ylmethyl)-1*H*-indole-2,3-dione-3-(*N*-allylthiosemicarbazone) (3f). Orange powder (87%): mp 145–147 °C; IR (KBr): υ 3211 (NH), 1696 (C=O), 1145 (C=S); ^{1}H NMR (DMSO-d_6/400 MHz): δ 1.33 (br s, 2H, pip. C_4–H_2), 1.46 (br s, 4H, pip. C_3–H_2, C_5–H_2), 2.51 (s, DMSO, pip. C_2–H_2, C_6–H_2), 4.27 (t, J = 5.43 Hz, 2H, allyl C_1–H_2), 4.46 (s, 2H, N–CH_2–N), 5.16 (dd, J = 10.19, 1.04 Hz, 1H, allyl C_3–H_{cis}), 5.24 (dd, J = 17.23, 1.23 Hz, 1H, allyl C_3–H_{trans}), 5.88–5.96 (m, 1H, allyl C_2–H), 7.25 (d, J = 5.87 Hz, 2H, indole C_7–H, C_6–H), 7.55 (d, J = 7.95 Hz, 1H, indole C_4–H), 9.55 (t, J = 5.84 Hz, 1H, N_4–H), 12.41 (s, 1H, N_2–H). Anal. Calcd for $C_{18}H_{22}FN_5OS$ (375.46): C, 57.58; H, 5.91; N, 18.65. Found: C, 57.71; H, 5.80; N, 18.60.

4.3.7. 5-Fluoro-1-(morpholin-4-ylmethyl)-1*H*-indole-2,3-dione-3-(*N*-butylthiosemicarbazone) (3g). Dark yellow powder (75%): mp 140–141 °C; IR (KBr): υ 3216 (NH), 1701 (C=O), 1130 (C=S); ^{1}H NMR (DMSO-d_6/500 MHz): δ 0.94 (t, J = 7.25 Hz, 3H, butyl CH_3), 1.35–1.38 (m, 2H, butyl C_3–H_2), 1.63 (p, J = 7.05 Hz, 2H, butyl C_2–H_2), 2.56 (t, J = 4.03 Hz, 4H, morph. C_3–H_2, C_5–H_2), 3.55 (t, J = 4.23 Hz, 4H, morph. C_2–H_2, C_6–H_2), 3.63 (q, J = 6.84 Hz, 2H, butyl C_1–H_2), 4.49 (s, 2H, N–CH_2–N), 7.27–7.29 (m, 2H, indole C_7–H, C_6–H), 7.57 (dd, J = 7.45, 2.21 Hz, 1H, indole C_4–H), 9.36 (t, J = 5.84 Hz, 1H, N_4–H), 12.36 (s, 1H, N_2–H); ^{13}C NMR (APT DMSO-d_6/100 MHz): δ 14.21 (butyl CH_3), 20.06 (butyl C_3), 30.96 (butyl C_2), 44.42 (butyl C_1), 50.96 (morph. C_3, C_5), 61.81 (N–CH_2–N), 66.45 (morph. C_2, C_6), 107.90 (d, J = 25.8 Hz, indole C_4),

112.76 (d, J = 7.95 Hz, indole C_7), 117.45 (d, J = 24.1 Hz, indole C_6), 121.30 (d, J = 9.44 Hz, indole C_{3a}), 130.22 (d, J = 3.37 Hz, indole C_{7a}), 140.05 (d, J = 1.28 Hz, indole C_3), 159.13 (d, J = 238.50 Hz, indole C_5), 162.06 (indole C═O), 177.30 (C═S). LCMS-APCI (−/+): m/z (%) 392 (MH^-, 100), 394 (MH^+, 100). Anal. Calcd for $C_{18}H_{24}FN_5O_2S$ (393.47): C, 54.94; H, 6.15; N, 17.80. Found: C, 54.87; H, 6.04; N, 17.84.

4.3.8. 5-Fluoro-1-(piperidin-1-ylmethyl)-1*H*-indole-2,3-dione-3-(*N*-butylthiosemicarbazone) (3h). Dark yellow powder (88%): mp 145–146 °C; IR (KBr): υ 3214 (NH), 1697 (C═O), 1143 (C═S); ^{1}H NMR (DMSO-d_6/500 MHz): δ 0.93 (t, J = 7.35 Hz, 3H, butyl CH_3), 1.33–1.38 (m, 4H, pip. C_4–H_2, butyl C_3–H_2), 1.46 (br s, 4H, pip. C_3–H_2, C_5–H_2), 1.63 (p, J = 7.35 Hz, 2H, butyl C_2–H_2), 2.51–2.52 (m, DMSO, pip. C_2–H, C_6–H), 3.63 (q, J = 6.92 Hz, 2H, butyl C_1–H_2), 4.48 (s, 2H, N–CH_2–N), 7.26–7.27 (m, 2H, indole C_7–H, C_6–H), 7.56 (dd, J = 7.83, 1.11 Hz, 1H, indole C_4–H), 9.35 (t, J = 5.75 Hz, 1H, N_4–H), 12.38 (s, 1H, N_2–H); ^{13}C NMR (APT DMSO-d_6/100 MHz): δ 14.20 (butyl CH_3), 20.04 (butyl C_3), 24.00 (pip. C_4), 25.80 (pip. C_3, C_5), 30.94 (butyl C_2), 44.41 (butyl C_1), 51.78 (pip. C_2, C_6), 62.50 (N–CH_2–N), 107.87 (d, J = 25.7 Hz, indole C_4), 112.86 (d, J = 7.73 Hz, indole C_7), 117.49 (d, J = 23.9 Hz, indole C_6), 121.20 (d, J = 9.30 Hz, indole C_{3a}), 130.28 (indole C_{7a}), 140.34 (indole C_3), 159.06 (d, J = 238.4 Hz, indole C_5), 162.09 (indole C═O), 177.29 (C═S). Anal. Calcd for $C_{19}H_{26}FN_5OS$ (391.50): C, 58.29; H, 6.69; N, 17.89. Found: C, 57.85; H, 6.80; N, 17.82.

4.3.9. 5-Fluoro-1-(morpholin-4-ylmethyl)-1*H*-indole-2,3-dione-3-(*N*-cyclohexylthiosemicarbazone) (3i). Yellow powder (93%): mp 176–177 °C; IR (KBr): υ 3220 (NH),1695 (C═O), 1135 (C═S); ^{1}H NMR (DMSO-d_6/400 MHz): δ 1.16 (t, J = 12.58 Hz, 1H, cycl. C_4–H_{ax}), 1.26–1.35 (m, 2H, cycl. C_3–H_{ax}, C_5–H_{ax}), 1.42–1.52 (m, 2H, cycl. C_2–H_{ax}, C_6–H_{ax}), 1.64 (d, J = 12.43 Hz, 1H, cycl. C_4–H_{equiv}), 1.78 (d, J = 12.98 Hz, 2H, cycl. C_3–H_{equiv}, C_5–H_{equiv}), 1.93 (d, J = 9.94 Hz, 2H, cycl. C_2–H_{equiv}, C_6–H_{equiv}), 2.55 (t, J = 4.01 Hz, 4H, morph. C_3–H_2, C_5–H_2), 3.54 (t, J = 4.22 Hz, 4H, morph. C_2–H_2, C_6–H_2), 4.18–4.22 (m, 1H, cycl. C_1–H), 4.49 (s, 2H, N–CH_2–N), 7.26–7.29 (m, 2H, indole C_7–H, C_6–H), 7.69 (dd, J = 7.42, 1.38 Hz, 1H, indole C_4–H), 8.92 (d, J = 8.52 Hz, 1H, N_4–H), 12.39 (s, 1H, N_2–H). Anal. Calcd for $C_{20}H_{26}FN_5O_2S$ (419.51): C, 57.26; H, 6.25; N, 16.69. Found: C, 57.56; H, 6.15; N, 16.76.

4.3.10. 5-Fluoro-1-(morpholin-4-ylmethyl)-1*H*-indole-2,3-dione-3-(*N*-benzylthiosemicarbazone) (3j). Orange powder (96%): mp 171–172 °C; IR (KBr): υ 3247 (NH), 1691 (C═O), 1139 (C═S); ^{1}H NMR (DMSO-d_6/500 MHz): δ 2.57 (t, J = 4.42 Hz, 4H, morph. C_3–H_2, C_5–H_2), 3.55 (t, J = 4.42 Hz, 4H, morph. C_2–H_2, C_6–H_2), 4.50 (s, 2H, N–CH_2–N), 4.91 (d, J = 6.10 Hz, 2H, benzyl CH_2), 7.27–7.39 (m, 7H, indole C_7–H, C_6–H, phenyl), 7.56 (dd, J = 7.94, 1.97 Hz, 1H, indole C_4–H), 9.93 (t, J = 6.30 Hz, 1H, N_4–H), 12.47 (s, 1H, N_2–H). Anal. Calcd for $C_{21}H_{22}FN_5O_2S$ (427.49): C, 59.00; H, 5.19; N, 16.38. Found: C, 59.05; H, 5.09; N, 16.45.

4.3.11. 5-Fluoro-1-(piperidin-1-ylmethyl)-1*H*-indole-2,3-dione-3-(*N*-benzylthiosemicarbazone) (3k). Orange powder (98%): mp 177 °C; IR (KBr): υ 3270 (NH), 1690 (C═O), 1158 (C═S); ^{1}H NMR (DMSO-d_6/500 MHz): δ 1.34 (br s, 2H, pip. C_4–H_2), 1.47 (br p, J = 5.18 Hz, 4H, pip. C_3–H_2, C_5–H_2), 2.51–2.53 (m, DMSO, pip. C_2–H_2, C_6–H_2), 4.49 (s, 2H, N–CH_2–N), 4.91 (d, J = 6.10 Hz, 2H, benzyl CH_2), 7.27–7.39 (m, 7H, indole C_7–H, C_6–H, phenyl), 7.55 (dd, J = 7.32, 2.13 Hz, 1H, indole C_4–H), 9.92 (t, J = 6.30 Hz, 1H, N_4–H), 12.49 (s, 1H, N_2–H). Anal. Calcd for $C_{22}H_{24}FN_5OS$ (425.52): C, 62.10; H, 5.68; N, 16.46. Found: C, 61.79; H, 5.47; N, 16.33.

4.3.12. 5-Fluoro-1-(morpholin-4-ylmethyl)-1*H*-indole-2,3-dione-3-(*N*-phenylthiosemicarbazone) (3l). Orange powder (92%): mp 179 °C; IR (KBr): υ 3308, 3218 (NH), 1689 (C═O), 1155 (C═S); ^{1}H NMR (DMSO-d_6/500 MHz): δ 2.58 (t, J = 4.42 Hz, 4H, morph. C_3–H_2, C_5–H_2), 3.55 (t, J = 4.57 Hz, 4H, morph. C_2–H_2, C_6–H_2), 4.51 (s, 2H, N–CH_2–N), 7.28–7.31(m, 3H, indole C_7–H, C_6–H, phenyl C_4–H), 7.45 (dd, J = 7.93, 1.83 Hz, 2H, phenyl C_3–H, C_5–H), 7.62 (d, J = 8.53 Hz, 2H, phenyl C_2–H, C_6–H), 7.71 (dd, J = 8.69, 1.62 Hz, 1H, indole C_4–H), 10.88 (s, 1H, N_4–H), 12.58 (s, 1H, N_2–H). Anal. Calcd for $C_{20}H_{20}FN_5O_2S{\cdot}1/2H_2O$ (422.47): C, 56.85; H, 5.01; N, 16.57. Found: C, 56.27; H, 5.14; N, 16.05.

4.3.13. 5-Fluoro-1-(piperidin-1-ylmethyl)-1*H*-indole-2,3-dione-3-(*N*-phenylthiosemicarbazone) (3m). Dark yellow powder (98%): mp 174–175 °C; IR (KBr): υ 3285, 3215 (NH), 1692 (C═O), 1135 (C═S); ^{1}H NMR (DMSO-d_6/500 MHz): δ 1.34 (br s, 2H, pip. C_4–H_2), 1.47 (br p, J = 5.41 Hz, 4H, pip. C_3–H_2, C_5–H_2), 2.54 (br t, J = 4.88 Hz, 4H, pip. C_2–H_2, C_6–H_2), 4.49 (s, 2H, N–CH_2–N), 7.27–7.31 (m, 3H, indole C_7–H, C_6–H, phenyl C_4–H), 7.44 (t, J = 7.93 Hz, 2H, phenyl C_3–H, C_5–H), 7.62 (d, J = 8.07 Hz, 2H, phenyl C_2–H, C_6–H), 7.70 (d, J = 7.62 Hz, 1H, indole C_4–H), 10.87 (s, 1H, N_4–H), 12.60 (s, 1H, N_2–H); LCMS-APCI (−/+): m/z (%) 410 (MH^-, 10), 178 (100), 412 (MH^+, 12), 180 (100). Anal. Calcd for $C_{21}H_{22}FN_5OS$ (411.49): C, 61.29; H, 5.38; N, 17.01. Found: C, 61.32; H, 5.61; N, 16.95.

4.3.14. 5-Fluoro-1-(piperidin-1-ylmethyl)-1*H*-indole-2,3-dione-3-[*N*-(4-methylphenyl)thiosemicarbazone] (3n). Orange powder (89%): mp 161–162 °C; IR (KBr): υ 3291, 3215 (NH), 1689 (C═O), 1145 (C═S); ^{1}H NMR (DMSO-d_6/500 MHz): δ 1.35 (br s, 2H, pip. C_4–H_2), 1.47 (br p, J = 5.40 Hz, 4H, pip. C_3–H_2, C_5–H_2), 2.34 (s, 3H, CH_3), 2.54 (br t, J = 4.88 Hz, 4H, pip. C_2–H_2, C_6–H_2), 4.49 (s, 2H, N–CH_2–N), 7.24 (d, J = 8.54 Hz, 2H, phenyl C_3–H, C_5–H), 7.27–7.29 (m, 2H, indole C_7–H, C_6–H), 7.48 (d, J = 8.24 Hz, 2H, phenyl C_2–H, C_6–H), 7.69 (dd, J = 8.24, 1.22 Hz, 1H, indole C_4–H), 10.81 (s, 1H, N_4–H), 12.58 (s, 1H, N_2–H); LCMS-APCI (−/+): m/z (%) 426 (MH^+, 10), 329 (100). Anal. Calcd for $C_{22}H_{24}FN_5OS$ (425.52): C, 62.10; H, 5.68; N, 16.46. Found: C, 61.98; H, 6.00; N, 16.48.

4.3.15. 5-Fluoro-1-(morpholin-4-ylmethyl)-1*H*-indole-2,3-dione-3-[*N*-(4-chlorophenyl)thiosemicarbazone] (3o). Dark yellow powder (98%): mp 185–187 °C; IR (KBr): υ 3308, 3220 (NH), 1690 (C=O), 1140 (C=S); ^{1}H NMR (DMSO-d_6/400 MHz): δ 2.57 (br s, 4H, morph. C_3–H_2, C_5–H_2), 3.55 (t, J = 4.17 Hz, 4H, morph. C_2–H_2, C_6–H_2), 4.51 (s, 2H, N–CH_2–N), 7.31 (d, J = 6.81 Hz, 2H, indole C_7–H, C_6–H), 7.51 (d, J = 8.69 Hz, 2H, phenyl C_3–H, C_5–H), 7.67 (d, J = 8.59 Hz, 2H, phenyl C_2–H, C_6–H), 7.68 (d, J = 6.50 Hz, 1H, indole C_4–H), 10.93 (s, 1H, N_4–H), 12.62 (s, 1H, N_2–H). Anal. Calcd for $C_{20}H_{19}ClFN_5O_2S$ (447.91): C, 53.63; H, 4.28; N, 15.64. Found: C, 53.19; H, 4.57; N, 15.47.

4.3.16. 5-Fluoro-1-(piperidin-1-ylmethyl)-1*H*-indole-2,3-dione-3-[*N*-(4-chlorophenyl)thiosemicarbazone] (3p). Yellow powder (93%): mp 178–179 °C; IR (KBr): υ 3301, 3237 (NH), 1698 (C=O), 1140 (C=S); ^{1}H NMR (DMSO-d_6/400 MHz): δ 1.34 (br s, 2H, pip. C_4–H_2), 1.47 (br s, 4H, pip. C_3–H_2, C_5–H_2), 2.53 (br s, 4H, pip. C_2–H_2, C_6–H_2), 4.50 (s, 2H, N–CH_2–N), 7.30 (dd, J = 7.37, 1.70 Hz, 2H, indole C_7–H, C_6–H), 7.51 (d, J = 8.79 Hz, 2H, phenyl C_3–H, C_5–H), 7.65–7.68 (m, 3H, phenyl C_2–H, C_6–H, indole C_4–H), 10.92 (s, 1H, N_4–H), 12.65 (s, 1H, N_2–H). Anal. Calcd for $C_{21}H_{21}ClFN_5OS$. 1/2H_2O (454.95): C, 55.44; H, 4.87; N, 15.39. Found: C, 55.38; H, 4.89; N, 15.48.

4.3.17. 5-Fluoro-1-(morpholin-4-ylmethyl)-1*H*-indole-2,3-dione-3-[*N*-(4-fluorophenyl)thiosemicarbazone] (3q). Dark yellow powder (67%). mp 167–168 °C; IR (KBr): υ 3309, 3288 (NH), 1689 (C=O), 1138 (C=S); ^{1}H NMR (DMSO-d_6/500 MHz): δ 2.57 (t, J = 4.39 Hz, 4H, morph. C_3–H_2, C_5–H_2), 3.55 (t, J = 4.39 Hz, 4H, morph. C_2–H_2, C_6–H_2), 4.51 (s, 2H, N–CH_2–N), 7.26–7.31 (m, 4H, indole C_7–H, C_6–H, phenyl C_3–H, C_5–H), 7.61 (dd, J = 8.79, 4.88 Hz, 2H, phenyl C_2–H, C_6–H), 7.68 (dd, J = 7.32, 1.46 Hz, 1H, indole C_4–H), 10.88 (s, 1H, N_4–H), 12.59 (s, 1H, N_2–H); LCMS-APCI (−/+): m/z (%) 430 (MH^-, 2), 331 (100). Anal. Calcd for $C_{20}H_{19}F_2N_5O_2S$ (431.45): C, 55.67; H, 4.44; N, 16.23. Found: C, 55.31; H, 4.00; N, 15.90.

4.3.18. 5-Fluoro-1-(piperidin-1-ylmethyl)-1*H*-indole-2,3-dione-3-[*N*-(4-fluorophenyl)thiosemicarbazone] (3r). Dark yellow powder (74%): mp 149–151 °C; IR (KBr): υ 3305, 3230 (NH), 1697 (C=O), 1137 (C=S); ^{1}H NMR (DMSO-d_6/500 MHz): δ 1.35 (br s, 2H, pip. C_4–H_2), 1.48 (br p, J = 5.25 Hz, 4H, pip. C_3–H_2, C_5–H_2), 2.54 (t, J = 4.69 Hz, 4H, pip. C_2–H, C_6–H), 4.50 (s, 2H, N–CH_2–N), 7.27–7.30 (m, 4H, indole C_7–H, C_6–H, phenyl C_3–H, C_5–H), 7.62 (dd, J = 9.06, 5.03 Hz, 2H, phenyl C_2–H, C_6–H), 7.67 (d, J = 8.05 Hz, 1H, indole C_4–H), 10.88 (s, 1H, N_4–H), 12.62 (s, 1H, N_2–H). Anal. Calcd for $C_{21}H_{21}F_2N_5OS$ (429.48): C, 58.73; H, 4.93; N, 16.31. Found: C, 58.40; H, 4.70; N, 16.74.

4.4. General method for the synthesis of 5-nitro-1-morpholino/piperidinomethyl-1*H*-indole-2,3-dione-3-thiosemicarbazones (4a–l)[19]

To a suspension of **2l–v** (2 mmol) in absolute ethanol (20 mL), 37% formaldehyde solution (0.5 mL) and morpholine or piperidine (2 mmol) were added dropwise with vigorous stirring. After combining all reagents, the reaction mixture was refluxed on a water bath for 4 h. The product formed was filtered and washed with petroleum ether.

4.5. General method for the synthesis of 5-nitro-1*H*-indole-2,3-dione-3-[(4-oxo-1,3-thiazolidin-2-ylidene)-hydrazones] (5a–s)[20]

To a suspension of **2l–v** (2.5 mmol) in absolute ethanol (25 mL), anhydrous sodium acetate (1 mmol) and ethyl bromoacetate or ethyl 2-bromopropionate (2.5 mmol) were added. The reaction mixture was refluxed for 4 h, cooled, diluted with water, and allowed to stand overnight. The yellow crystals obtained were filtered and purified by recrystallization from ethanol.

4.6. Single crystal X-ray structure determinations

Specimens of **3e** and **3f** of suitable quality and size were mounted on the ends of glass and used for the intensity data collection. The X-ray diffraction data on **3e** and **3f** were collected using an automatic X-ray four-circle EXCALIBUR single crystal diffractometer with CCD area detectors. Graphite monochromated Mo Kα radiation (λ = 0.71073 Å) was generated at 50 kV and 40 mA. The intensities of the reflections were recorded in 104 frames (each frame consisting of 1024 × 1024 pixels with 2 × 2 pixels bining) for both crystals. The lattice parameters were calculated from refinement of positions of all measured reflections. The data sets were corrected for Lorentz and polarization effect. No absorption correction was applied for both crystals.

Both structures were solved by direct methods program SHELXS-97[41] and refined by the full-matrix least-squares method based on F^2 using SHELXL-97.[42] All non-hydrogen atoms were refined with anisotropic displacement factors. N4 and N5 hydrogen atoms were positioned from difference map, and redundant hydrogen atoms were positioned geometrically and refined using a riding model. The geometric calculations were carried out with the Platon[43] program.

4.7. In vitro evaluation of antituberculosis activity

The primary screen was conducted at 6.25 μg/mL (or molar equivalent of highest molecular weight compound in a series of congeners) against *Mycobacterium tuberculosis* H37Rv (ATCC 27294) in BACTEC 12B medium using a broth microdilution assay, the Microplate Alamar Blue Assay (MABA). Compounds exhibiting fluorescence were tested in the BACTEC 460 radiometric system.[25] Compounds effecting <90% inhibition in the primary screen (MIC > 6.25 μg/mL) were not generally evaluated further. Compounds demonstrating at least 90% inhibition in the primary screen were re-tested at lower concentrations against *M. tuberculosis* H37Rv to determine the actual minimum inhibitory concentration (MIC) in the MABA. The MIC was defined as the lowest concentration effecting the reduction in fluorescence of 90% relative to controls. Concurrent with the deter-

mination of MICs, compounds were tested for cytotoxicity (IC_{50}) in VERO cells at concentrations 10× the MIC for *M. tuberculosis* H37Rv.

4.7.1. Microplate Alamar Blue Assay (MABA). Antimicrobial susceptibility testing was performed in black, clear-bottomed, 96-well microplates (black view plates; Packard Instrument Company, Meriden, Conn.) in order to minimize background fluorescence. Outer perimeter wells were filled with sterile water to prevent dehydration in experimental wells. Initial drug dilutions were prepared in either dimethylsulfoxide or distilled deionized water, and subsequent twofold dilutions were performed in 0.1 mL of 7H9GC (no Tween 80) in the microplates. BACTEC 12B-passaged inocula were initially diluted 1:2 in 7H9GC, and 0.1 mL was added to wells. The determination of bacterial titer yielded 1×10^6 CFU/ml in plate well for $H_{37}Rv$. Frozen inocula were initially diluted 1:20 in BACTEC 12B medium followed by a 1:50 dilution in 7H9GC. Addition of 1/10 mL to wells resulted in final bacterial titer of 20×10^5 CFU/ml for $H_{37}Rv$. Wells containing drug only were used to detect autofluorescence of compounds. Additional control wells consisted of bacteria only (B) and medium only (M). Plates were incubated at 37 °C. Starting at day 4 of incubation, 20 μL of 10× Alamar Blue solution (Alamar Biosciences/Accumed, Westlake, Ohio) and 12.5 μL of 20% Tween 80 were added to one B well and one M well, and plates were reincubated at 37 °C. Wells were observed 12 and 24 h later for a color change from blue to pink and for a reading of $\geqslant$50,000 fluorescence units (FU). Fluorescence was measured in a Cytofluor II microplate fluorometer (PerSeptive Biosystems, Framingham, Mass.) in bottom-reading mode with excitation at 530 nm and emission at 590 nm. If the B wells become pink after 24 h, the reagent is being added to the entire plate. If the well remains blue or $\geqslant$50,000 FU is measured, additional M and B wells are tested daily until a color change occurred, at which time reagents are added to all remaining wells. Plates were then incubated at 37 °C, and results were recorded at 24 h post-reagent addition. Visual MICs were defined as the lowest concentration of drug that prevented a color change. For fluorometric MICs, a background subtraction was performed on all wells with a mean of triplicate M wells. Percent inhibition was defined as (1 − (test well FU/mean FU of triplicate B wells) × 100). The lowest drug concentration effecting an inhibition of $\geqslant$90% was considered the MIC.

4.7.2. BACTEC radiometric assay. A total of 1/10 mL of BACTEC 12B-passaged inoculum was delivered without prior dilution into 4 mL of test medium. The determination of bacterial titer yielded average titer of 1×10^5 CFU/ml of BACTEC 12B medium for $H_{37}Rv$. Frozen inocula were initially diluted 1:20 in BACTEC 12B medium, and then 0.1 mL was delivered to the test medium. This yielded 5.0×10^5 CFU per BACTEC vial for $H_{37}Rv$. Twofold drug dilutions were prepared in either dimethylsulfoxide (DMSO) or distilled deionized water and delivered via a 0.5-mL insulin syringe in a 50-μL volume. Drug-free control vials consisted of solvent with bacterial inoculum and solvent with a 1:100 dilution of bacterial inoculum (1:100 controls). Vials were incubated at 37 °C, and the GI was determined in a BACTEC 460 instrument (Becton Dickinson) until the GI of the 1:100 controls reached at least 30. All vials were read the following day, and the GI and daily change in GI (ΔGI) were recorded for each drug dilution. The MIC was defined as the lowest concentration for which the ΔGI was less than the ΔGI of the 1:100 control. If the GI of the test sample was greater than 100, the sample was scored as resistant even if the ΔGI was less than the ΔGI of the 1:100 control.

Acknowledgments

We thank Dr. Joseph A. Maddry from the Tuberculosis Antimicrobial Acquisition and Coordinating Facility (TAACF), National Institute of Allergy and Infectious Diseases Southern Reserch Institute, Alabama, USA, for the evaluation of anti-TB activity. This work was supported by Istanbul University Research Fund, Project Numbers: 167/15012004 and BYP-484/30092004. The authors (FBK and SO) wish to acknowledge the support of Hacettepe University Research Fund (Project Number: 0302602001).

References and notes

1. Shinnick, T. M.; King, C. H.; Quinn, F. D. *Am. J. Med. Sci.* **1995**, *309*, 92.
2. Snider, D. E., Jr.; La Montagne, J. R. *J. Infect. Dis.* **1994**, *169*, 1189.
3. Pablos-Mendez, A.; Raviglione, M. C.; Laszlo, A.; Binkin, N.; Rieder, H. L.; Bustreo, F.; Cohn, D. L.; Lambregts-van Weezenbeek, C. S.; Kim, S. J.; Cahulet, P.; Nunn, P. *N. Eng. J. Med.* **1998**, *338*, 1641.
4. Houston, S.; Fanning, A. *Drugs* **1994**, *48*, 689.
5. Cocco, M. T.; Congiu, C.; Onnis, V.; Pellerano, M. L.; De Logu, A. *Bioorg. Med. Chem.* **2002**, *10*, 501.
6. Bermudez, L. E.; Reynolds, R.; Kolonoski, P.; Aralar, P.; Inderlied, C. B.; Young, L. S. *Antimicrob. Agents Chemother.* **2003**, *47*, 2685.
7. Logu, A. D.; Saddi, M.; Onnis, V.; Sanna, C.; Congiu, C.; Borgna, R.; Cocco, M. T. *Int. J. Antimicrob. Agents* **2005**, *26*, 28.
8. Sethi, M. L. Antiviral agents and protease inhibitors. In *Principles of Medicinal Chemistry*; Foye, W. O., Lemke, T. L., Williams, D. A., Eds.; Williams and Wilkins: Baltimore, 2002; p 952.
9. Sriram, D.; Perumal, Y. *Curr. Med. Chem.* **2003**, *10*, 1689.
10. Pirrung, M. C.; Pansare, S. V.; Das Sarma, K.; Keith, K. A.; Kern, E. R. *J. Med. Chem.* **2005**, *48*, 3045.
11. Bal, T. R.; Anand, B.; Yogeeswari, P.; Sriram, D. *Bioorg. Med. Chem. Lett.* **2005**, *15*, 4451.
12. Karalı, N.; Terzioğlu, N.; Gürsoy, A. *Arzneim.-Forsch./ Drug Res.* **1998**, *48*, 758.
13. Sriram, D.; Yogeeswari, P.; Gopal, G. *Eur. J. Med. Chem.* **2005**, *40*, 1373.
14. Pandeya, S. N.; Sriram, D.; Nath, G.; DeClercq, E. *Eur. J. Pharm. Sci.* **1999**, *9*, 25.
15. Pandeya, S. N.; Sriram, D.; Nath, G.; DeClercq, E. *Arzneim.-Forsch./ Drug Res.* **2000**, *50*.
16. Webber, S. E.; Tikhe, J.; Worland, S. T.; Fuhrman, S. A.; Hendrickson, T. F.; Matthews, D. A.; Love, R. A.; Patick,

A. K.; Meador, J. W.; Ferre, R. A.; Brown, E. L.; DeLisle, D. M.; Ford, C. E.; Binford, S. L. *J. Med. Chem.* **1996**, *39*, 5072.
17. Velezheva, V. S.; Brennan, P. J.; Marshakov, V. Y.; Gusev, D. V.; Lisichkina, I. N.; Peregudov, A. S.; Tchernousova, L. N.; Smirnova, T. G.; Andreevskaya, S. N.; Medvedev, A. E. *J. Med. Chem.* **2004**, *47*, 3455.
18. Badawy, M. A.; Abdel-Hady, S. A. *Arch. Pharm. (Weinheim)* **1991**, *324*, 349.
19. Karalı, N. *Eur. J. Med. Chem.* **2002**, *37*, 909.
20. Terzioğlu, N.; Karalı, N.; Gürsoy, A.; Pannecouque, C.; Leysen, P.; Paeshuyse, J.; Neyts, J.; De Clercq, E. *ARKIVOC* **2006**, *i*, 109.
21. Macaev, F.; Rusu, G.; Pogrebnoi, S.; Gudima, A.; Stingaci, E.; Vlad, L.; Shvets, N.; Kandemirli, F.; Dimoglo, A.; Reynolds, R. *Bioorg. Med. Chem.* **2005**, *13*, 4842.
22. Oruc, E. E.; Rollas, S.; Kandemirli, F.; Shvets, N.; Dimoglo, A. *J. Med. Chem.* **2004**, *47*, 6760.
23. Cremer, D.; Pople, J. A. *J. Am. Chem. Soc.* **1975**, *97*, 1354.
24. Umezawa, Y.; Tsuboyama, S.; Takahashi, H.; Uzawa, J.; Nishio, M. *Tetrahedron* **1999**, *55*, 10047.
25. Collins, L. A.; Franzblau, S. G. *Antimicrob. Agents Chemother.* **1997**, *41*, 1004.
26. MOPAC: *A General Molecular Orbital Package* (Version 6.0), Steward J.J.P. QCPE #455.
27. Dimoglo, A. S. *Khimiko-pharm. Zhurnal* **1985**, *4*, 438.
28. Shvets, N. M. *J. Comput. Sci. Moldova* **1993**, *1*, 101.
29. Bersuker, I. B.; Dimoglo, A. S. The Electron- Topological Approach to the QSAR Problem. In *Reviews in Computational Chemistry*; Lipkowitz, K. B.; Boyd, D. B., Eds.; VCH: New-York, 1991; Chapter 10.
30. Dimoglo, A. S.; Shvets, N. M.; Tetko, I. V.; Livingstone, D. J. *Quant. Struct.-Act. Relat.* **2001**, *20*, 31.
31. Shvets, N. M.; Dimoglo, A. S. *Nahrung* **1998**, *42*, 364.
32. Kandemirli, F.; Saraçoğlu, M.; Kovalishyn, V. *Mini Rev. Med. Chem.* **2005**, *5*, 479.
33. Kohonen, T. *Self-organisation Maps*; Springer: Berlin, 1995.
34. Bishop, M. *Neural Networks for Pattern Recognition*; Oxford University Press: Oxford, 1995.
35. Tetko, I. V. www.vcclab.org, 2005.
36. Dimoglo, A.; Kovalishyn, V.; Shvets, N.; Ahsen, V. *Mini Rev. Med. Chem.* **2005**, *5*, 879.
37. Kohonen, T.; Hinninen, J.; Kangas, J.; Laaksonen, J. SOM_PAK: The self-organizing map program package is obtainable via anonymous ftp from the internet address "cochlea.hut.fi" (130.233.168.48).
38. Tetko, I. V.; Livingstone, D. J.; Luik, A. I. *J. Chem. Inf. Comput. Sci.* **1995**, *35*, 826.
39. Tetko, I. V.; Villa, A. E. P.; Livingstone, D. J. *J. Chem. Inf. Comput. Sci.* **1996**, *36*, 794.
40. Kovalishyn, V. V.; Tetko, I. V.; Luik, A. I.; Kholodovych, V. V.; Villa, A. E. P.; Livingstone, D. J. *J. Chem. Inf. Comput. Sci.* **1998**, *38*, 651.
41. Sheldrick, G .M. SHELXS97. Program for crystal structure solution. University of Göttingen, Germany, 1997.
42. Sheldrick, G. M. SHELXL97. Program for crystal structure refinement. University of Göttingen, Germany, 1997.
43. Spek, A. L. *Acta Cryst.* **1990**, *A46*, C34.